mRNA vaccine-induced T cells respond identically to SARS-CoV-2 variants of concern but differ in longevity and homing properties depending on prior infection status

Jason Neidleman[1, 2, †], Xiaoyu Luo[1, †], Matthew McGregor[1, 2], Guorui Xie[1, 2], Victoria Murray[3], Warner C. Greene[1, 4], Sulggi A. Lee[5, *], and Nadia R. Roan[1, 2, *, #]

[1] Gladstone Institute of Virology, San Francisco, CA, USA

[2] Department of Urology, University of California, San Francisco, CA, USA

[3] Zuckerberg San Francisco General Hospital and the University of California, San Francisco, CA, USA

[4] Departments of Medicine, and Microbiology and Immunology, University of California, San Francisco, CA, USA

[†]Equal contribution

[*]Co-correspondence:

nadia.roan@gladstone.ucsf.edu, sulggi.lee@ucsf.edu

[#]Lead contact

ABSTRACT

While mRNA vaccines are proving highly efficacious against SARS-CoV-2, it is important to determine how booster doses and prior infection influence the immune defense they elicit, and whether they protect against variants. Focusing on the T cell response, we conducted a longitudinal study of infection-naïve and COVID-19 convalescent donors before vaccination and after their first and second vaccine doses, using a high-parameter CyTOF analysis to phenotype their SARS-CoV-2-specific T cells. Vaccine-elicited spike-specific T cells responded similarly to stimulation by spike epitopes from the ancestral, B.1.1.7 and B.1.351 variant strains, both in terms of cell numbers and phenotypes. In infection-naïve individuals, the second dose boosted the quantity and altered the phenotypic properties of SARS-CoV-2-specific T cells, while in convalescents the second dose changed neither. Spike-specific T cells from convalescent vaccinees differed strikingly from those of infection-naïve vaccinees, with phenotypic features suggesting superior long-term persistence and ability to home to the respiratory tract including the nasopharynx. These results provide reassurance that vaccine-elicited T cells respond robustly to emerging viral variants, confirm that convalescents may not need a second vaccine dose, and suggest that vaccinated convalescents may have more persistent nasopharynx-homing SARS-CoV-2-specific T cells compared to their infection-naïve counterparts.

INTRODUCTION

A year and a half since the December 2019 emergence of SARS-CoV-2, the novel betacoronavirus had already infected almost 200 million people and taken the lives of over 4 million, nearly collapsed worldwide health systems, disrupted the global economy, and perturbed society and public health on a scale not experienced within the past 100 years. Fortunately, multiple highly-efficacious vaccines, including the two-dose mRNA-based ones developed by Pfizer/BioNTech and Moderna, which confer ~90% protection against disease, were approved for emergency use before the end of 2020. Although the vaccines provide the most promising route for a rapid exit from the COVID-19 pandemic, concerns remain regarding the durability of the immunity elicited by these vaccines and the extent to which they will protect against the variants of SARS-CoV-2 now spreading rapidly around the world.

The first variant observed to display a survival advantage was the D614G, which was more transmissible than the original strain and quickly became the dominant variant throughout the world [1]. This variant, fortunately, did not evade immunity and in fact appeared to be more sensitive than the original strain to antibody neutralization by convalescent sera [2]. More worrisome, however, was the emergence at the end of 2020 of rapidly-spreading variants in multiple parts of the world, including B.1.1.7, B.1.351, P.1, and B.1.427/B.1.429 (originally identified in United Kingdom, South Africa, Brazil, and California, respectively) [3], followed by additional highly transmissible variants in 2021 including the B.1.61.72 which was first detected in India [4]. Some variants, including B.1.1.7, may be more virulent [5]. While antibodies against the original strain elicited by either vaccination or infection generally remain potent against B.1.1.7, their activity against B.1.351 and P.1 is compromised [6-15]. Antibodies from vaccinees were 14-fold less effective against B.1.351 than against the ancestral strain, and a subset of individuals completely lacked neutralizing antibody activity against B.1.351 9 months or more after convalescence [13].

Reassuringly, early data suggest that relative to antibody responses, T cell-mediated immunity appears to be less prone to evasion by the variants [16-22]. Among 280 CD4+ and 523

63 CD8+ T cell epitopes from the original SARS-CoV-2, an average of 91.5% (for CD4) and 98.1%
64 (for CD8) mapped to regions not mutated in the B.1.1.7, B1.351, P.1, and B.1.427/B.1.429
65 variants. Focusing on just the spike response, the sole SARS-CoV-2 antigen in the mRNA-based
66 vaccines, then 89.7% of the CD4+ epitopes and 96.4% of the CD8+ epitopes are conserved [17].
67 In line with this, the magnitude of the response of T cells from convalescent or vaccinated
68 individuals was not markedly reduced when assessed against any of the variants [17]. The relative
69 resistance of T cells against SARS-CoV-2 immune evasion is important in light of the critical role
70 these immune effectors play during COVID-19. T cell numbers display a strong, inverse
71 association with disease severity [23, 24], and the frequency of SARS-CoV-2-specific T cells predicts
72 recovery from severe disease [25, 26]. SARS-CoV-2-specific T cells can also provide long-term, self-
73 renewing immunological memory: these cells are detected more than half a year into
74 convalescence, and can proliferate in response to homeostatic signals [27, 28]. Furthermore, the
75 ability of individuals with inborn deficiencies in B cell responses to recover from COVID-19 without
76 intensive care suggests that the combination of T cells and innate immune mechanisms is
77 sufficient for recovery when antibodies are lacking [29].

78 Although T cells against the ancestral strain display a response of similar magnitude and
79 breadth to the variants [17], to what extent these T cells' phenotypes and effector functions differ
80 during their response to variant detection is a different question. Small changes in the sequences
81 of T cell epitopes, in the form of altered peptide ligands (APLs), can theoretically alter how the T
82 cells respond to stimulation. Indeed, change of a single residue can convert a proliferative, IL4-
83 secreting effector response into one that continues to produce IL4 in the absence of proliferation
84 [30]. Furthermore, APLs can activate Th1 cells without inducing either proliferation or cytokine
85 production, shift Th1 responses into Th2-focused ones, and in some instances even render T
86 cells anergic or immunoregulatory by eliciting TGFβ production [31].

87 Another important aspect that hasn't been explored is to what extent vaccine- vs. infection-
88 induced T cell responses differ phenotypically and functionally, and to what extent convalescent

89 individuals benefit from vaccination as they already harbor some form of immunity against the
90 virus. Studies based on the antibody and B cell response suggest that for COVID-19
91 convalescents, a single dose of the mRNA vaccines is helpful while the additional booster is not
92 necessary [10, 32, 33]; how this translates in the context of vaccine-elicited T cell immunity is not clear.
93 To address these knowledge gaps, we conducted 39-parameter phenotyping by CyTOF
94 on 33 longitudinal specimens from 11 mRNA-vaccinated individuals, 6 of whom had previously
95 contracted and recovered from COVID-19. For each participant, blood specimens were obtained
96 prior to vaccination, two weeks following the first dose, and two weeks following the second. For
97 every specimen, we assessed in depth the phenotypes and effector functions of total CD4+ and
98 CD8+ T cells, and of CD4+ and CD8+ T cells responding to the original SARS-CoV-2 spike, to
99 spike from variants B.1.1.7 and B.1.351, and to nucleocapsid. By conducting analyses on the
100 resulting 165 high-dimensional datasets generated, we find a reassuringly unaltered T cell
101 response against the variants, an ability of the booster dose to alter the phenotypes of vaccine-
102 elicited T cells, and a striking impact of prior infection on qualitative features of T cells elicited by
103 vaccination.
104
105 **RESULTS**
106 **Study Design**
107 To characterize the phenotypic features of mRNA vaccination-elicited SARS-CoV-2-
108 specific T cells, we procured 33 longitudinal blood samples from the COVID-19 Host Immune
109 Response and Pathogenesis (CHIRP) cohort. Four of the participants had received the
110 Moderna (mRNA-1273) vaccine, while the remaining 7 had received the Pfizer/BioNTech
111 (BNT162b2) one. For all participants, longitudinal specimens were obtained at three timepoints:
112 prior to vaccination, ~2 weeks (range 13-18 days) after the first vaccine dose, and ~2 weeks
113 (range 6-38 days) after the second dose. Five of the participants were never infected with
114 SARS-CoV-2, while the remaining 6 had completely recovered from mild (non-hospitalized)

115 COVID-19 disease (Table S1). These prior infections had all occurred in the San Francisco Bay
116 Area between March – July of 2020, when the dominant local strain was the original ancestral
117 strain. Each specimen was phenotyped using a 39-parameter T cell-centric CyTOF panel (see
118 Methods and Table S2) at baseline (to establish the overall phenotypes of total CD4+ and CD8+
119 T cells), and following 6 hours of stimulation with overlapping 15-mer peptides spanning the
120 entire original (ancestral) SARS-CoV-2-spike, B.1.1.7 spike, B.1.351 spike, or the original
121 SARS-CoV-2 nucleocapsid (the latter as a control for a SARS-CoV-2-specific response not
122 boosted by vaccination). Including all the baseline and stimulation conditions, a total of 165
123 specimens from the 11 participants were analyzed by CyTOF.
124
125 **SARS-CoV-2-specific T cells elicited by vaccination recognize B.1.1.7 and B.1.351**
126 **variants**
127 We first confirmed our ability to identify SARS-CoV-2-specific T cells by stimulating
128 PBMCs from vaccinated individuals with spike peptides. In line with our prior studies
129 implementing a 6-hour peptide stimulation [26, 28], spike-specific CD4+ T cells could be specifically
130 identified through intracellular cytokine staining for IFNγ, and a more robust response was
131 observed among CD4+ than CD8+ T cells (Fig. 1A). Activation induced markers (AIM) such as
132 Ox40, 4-1BB, and CD69 could also be identified in T cells after spike peptide stimulation, but
133 with a higher background in the baseline (no peptide stimulation) specimens relative to the
134 intracellular cytokine staining approach (Fig. S1). For this reason, in this study we exclusively
135 used IFNγ positivity in the peptide-stimulated samples as a marker of antigen-specific T cells.
136 In the infection-naïve participants, the first vaccination dose primed a spike-specific
137 CD4+ T cell response, which was further boosted with the second dose (Fig. 1B, *top left*). For
138 each participant and time point, similar numbers of cells were stimulated by exposure to the
139 ancestral or variant spikes. This finding suggests that vaccine-elicited spike-specific CD4+ T

140 cells recognize ancestral and variant spike equally well, and is consistent with their recently
141 reported ability to recognize variant strains [17]. The response of vaccine-elicited CD8+ T cells to
142 spike peptides was weaker, and mostly apparent only after the second dose (Fig. 1B, *top right*).
143 As expected, vaccination did not elicit T cells able to respond to nucleocapsid peptides (Fig. 1C,
144 *top panels*).

145 In contrast to the infection-naïve individuals where spike-specific CD4+ T cells were
146 clearly elicited and then boosted upon the second dose, spike-specific CD4+ T cell responses in
147 convalescent individuals did not show a consistent upward trend. Convalescent donor PID4112
148 had a large frequency of pre-vaccination SARS-CoV-2-specific CD4+ T cells that increased to
149 >1% of the total CD4+ T cell frequency after the first dose and then dampened after dose 2 (Fig.
150 1B, *bottom left*). PID4112 also exhibited an elevated nucleocapsid-specific CD4+ T cell
151 response after the first vaccination dose (Fig. 1C, *bottom left*), which may have been due to
152 bystander effects resulting from the concomitant large spike-specific response. In comparison,
153 PID4112's spike-specific CD8+ T cell response was low after dose 1, and boosted after dose 2
154 (Fig. 1B, *bottom right*). In contrast to PID4112, the remaining five convalescent donors exhibited
155 an overall weak spike-specific T cell response. In fact, when comparing these five donors to the
156 five infection-naïve donors, there was a significant decrease in the magnitude of the spike-
157 specific CD4+ T cell response, while the spike-specific CD8+ T cell response was equivalent
158 between the two groups (Fig. 1D). These results were unexpected and suggest that, when
159 excluding outlier PID4112, the magnitude of the vaccine-elicited spike-specific CD4+ T cell
160 response (after full vaccination) was lower in convalescent individuals than in infection-naïve
161 individuals.

162 These assessments of the magnitude of the spike-specific T cell response together
163 suggest that 1) in infection-naïve individuals the CD4+ T cell response is boosted by the second
164 vaccination dose, 2) convalescent individuals exhibit a more disparate response, with most
165 donors mounting a weaker response than infection-naïve individuals, and 3) the response is

166 more robust among CD4+ than CD8+ T cells. As a higher number of SARS-CoV-2-specific
167 CD4+ T cells were available for analysis, we focused on this subset for our subsequent
168 analyses.
169
170 **Vaccine-elicited spike-specific CD4+ T cells responding to B.1.1.7 and B.1.351 spike are**
171 **indistinguishable from those responding to ancestral spike**
172 Leveraging our ability to not only assess the magnitude but also the detailed (39-
173 parameter) phenotypic features of SARS-CoV-2-specific CD4+ T cells, we first determined
174 whether the ancestral and variant spike epitopes stimulated different subsets of vaccine-elicited
175 spike-specific CD4+ T cells. Such differences could theoretically result from the fact that ~5-
176 10% of the spike epitopes differ between variants and ancestral strains [17], and may therefore
177 act as APLs steering responding cells towards different fates. We isolated the datasets
178 corresponding to both post-vaccination timepoints for all eleven donors, and then exported the
179 data corresponding to spike-specific CD4+ T cells (as defined by IFNγ production, Fig. 1). After
180 reducing the multidimensional single-cell data for each individual specimen to a two-dimensional
181 datapoint through multidimensional scaling (MDS) [34], we observed the ancestral spike-
182 stimulated samples to be interspersed among the B.1.1.7- and B.1.351-responding ones (Fig.
183 2A). We then visualized the spike-specific CD4+ T cells at the single-cell level. When visualized
184 alongside total (baseline) CD4+ T cells, spike-specific cells occupied a distinct "island" defined
185 by high expression of IFNγ (Fig. 2B), suggesting unique phenotypic features of these cells. To
186 better analyze these spike-responding CD4+ T cells, we visualized them in isolation within a
187 new t-SNE which clearly demonstrated complete mixing of the cells stimulated by the ancestral,
188 B.1.1.7, and B.1.351 spike proteins (Fig. 2C). Almost all of the responding cells expressed high
189 levels of CD45RO and low levels of CD45RA (Fig. 2D), suggesting them to be mostly memory
190 cells. These memory CD4+ T cells included central memory T cells (Tcm), T follicular helper

191 cells (Tfh), and those expressing multiple activation markers (CD38, HLADR, CD69, CD25) and
192 receptors known to direct cells to tissues including the respiratory tract (CXCR4, CCR5, CCR6,
193 CD49d) (Fig. 2E). The expression levels of these and all other antigens quantitated by CyTOF
194 were not statistically different between CD4+ T cells responding to the three spike proteins (Fig.
195 S2). To confirm the identical phenotypes of the three groups of spike-responding cells, we
196 implemented unbiased clustering by flowSOM. Spike-stimulated cells were clustered into 8
197 subsets, and no subset was preferentially enriched in any one of the three groups (Fig. 2F).
198 Together, these data suggest that vaccine-elicited spike-specific CD4+ T cells respond in the
199 same manner to spike epitopes from the ancestral or variant strains, and would probably mount
200 similar responses *in vivo* to infection by all three virus types.
201
202 **Phenotypic alterations of spike-specific CD4+ T cells in infection-naïve recipients after**
203 **the second vaccine dose**
204 We next took advantage of our longitudinal study design to assess for any changes in
205 the differentiation of spike-specific T cell responses over the course of the 2-dose vaccination.
206 As the data presented above suggested no phenotypic differences between CD4+ T cells
207 responding to the ancestral, B.1.1.7, and B.1.351 spike proteins, our subsequent analyses
208 combined these datasets. We first assessed whether, among infection-naïve individuals, the
209 phenotypes of spike-specific CD4+ T cells were different after the first and second doses. While
210 MDS and tSNE visualizations of the data revealed that the cells from the two timepoints were
211 somewhat interspersed (Fig. 3A, B), flowSOM clustering suggested some differences in cluster
212 distribution (Fig. 3C, D). Direct comparison of the cluster frequencies revealed a cluster (B8)
213 significantly enriched after the first dose, and a different cluster (B5) significantly enriched after
214 the second dose (Fig. 3E). As these two clusters differentially expressed the Tcm markers
215 CD27 and CCR7 (Fig. 3F), we then assessed whether Tcm cells were differentially represented
216 among spike-specific CD4+ T cells after each of the vaccination doses. Indeed, Tcm cells were

217 significantly higher after the first dose (Fig. 3G), consistent with Cluster 8 (enriched after the first
218 dose) expressing high levels of these two receptors. Assessment of other canonical CD4+ T cell
219 subsets – in particular naïve (Tn), stem cell memory (Tscm), effector memory RA (Temra),
220 effector memory (Tem), T transitional memory (Ttm), Tfh, and regulatory T cells (Treg) –
221 revealed Tn cells, like the Tcm subset, to be decreased after the second dose. By contrast, Ttm
222 cells were found to be higher after the second dose, while the remaining subsets were not
223 altered (Fig. 3G, H). Overall, Tcm and Tfh were the most abundant subsets among the spike-
224 specific CD4+ T cells (Fig. 3G, H). These data together suggest that after receiving the second
225 dose, infection-naïve individuals' spike-specific CD4+ T cells increase in quantity (Fig. 1B), and
226 alter their phenotypes as reflected by a decrease Tcm cells and an increase in Ttm cells.
227 We then conducted a similar analysis in the convalescent individuals. As the pre-
228 vaccination timepoint included spike-specific CD4+ T cells primed by prior SARS-CoV-2
229 infection, we included all three timepoints in this analysis. When the data were visualized by
230 MDS, it was apparent that most of the pre-vaccination specimens localized away from the post-
231 vaccination specimens, which were interspersed with each other (Fig. 4A). Similar distinctions
232 between pre-and post-vaccination specimens were visualized at the single-cell level by tSNE,
233 which was particularly apparent when visualized as contour heatmaps (Fig. 4B, C). Clustering of
234 the cells by flowSOM revealed that the cluster distribution was markedly skewed among the pre-
235 vaccination cells (Fig. 4D, E), with one cluster being under-represented (C2) and one over-
236 represented (C5) as compared to both post-vaccination timepoints (Fig. 4F). Cluster C3 was the
237 only cluster that was significantly different after 1 vs. 2 doses (Fig. 4F) but as this cluster
238 comprised only < 5% of the cells it was not analyzed further. To assess what may drive the
239 differences between the phenotypes of the pre- vs. post-vaccination spike-specific CD4+ T
240 cells, we assessed for markers differentially expressed between clusters C2 and C5. Cluster C2
241 cells preferentially expressed the Tcm markers CD27 and CCR7, the Tfh markers PD1 and
242 CXCR5, and the co-stimulatory receptors ICOS and Ox40, while among these only CD27 was

243 preferentially expressed in Cluster C5 (Fig. S3). Manual gating confirmed Tcm, Tfh, and
244 ICOS+Ox40+ cells to be preferentially enriched in the post-vaccination specimens (Fig. 4G, H,
245 I). None of the canonical subsets were differentially abundant after the first vs. second
246 vaccination dose. Together, these results suggest that, in contrast to the infection-naïve
247 individuals, convalescents' spike-specific CD4+ T cells were similar after the first vs. second
248 vaccination dose; however, in these individuals vaccination drastically altered the phenotypes of
249 the pre-existing spike-specific CD4+ T cells (presumably elicited from the original infection).
250

251 **Vaccination-induced spike-specific CD4+ T cells from convalescent individuals exhibit**
252 **unique phenotypic features of increased longevity and tissue homing**

253 We next determined whether there were any phenotypic differences between the
254 vaccine-induced spike-specific CD4+ T cells from the infection-naïve vs. convalescent
255 individuals. Removal of convalescent outlier PID4112 revealed the magnitude of the spike-
256 specific CD4+ T cell response to be lower in the convalescents than in infection-naïve
257 participants after full vaccination (Fig. 1D). But when all donors were included there was no
258 statistically significant difference in response magnitude (Fig. 5A). However, the spike-specific
259 CD4+ T cells from the convalescent and infection-naïve individuals exhibited clear phenotypic
260 differences when assessed by both MDS (Fig. 5B) and tSNE contours (Fig. 5C); this was more
261 apparent after the second vaccine dose, but could already be observed after the first. Since the
262 cells after the second dose are more clinically relevant (as they are the ones persisting in
263 vaccinated individuals moving forward), we focused our subsequent analysis on just this
264 timepoint. When visualized as a dot plot, it was apparent that the spike-specific CD4+ T cells
265 from infection-naïve individuals segregated away from those from the convalescents (Fig. 5D).
266 Clustering of the data also demonstrated differences between the two patient groups (Fig. 5E,
267 F), which was confirmed by demonstration of a significant difference in Cluster A1 abundance
268 (Fig. 5G).

269 To identify these phenotypic differences, we first assessed the relative distributions of
270 the main canonical CD4+ T cell subsets. Interestingly, the vaccinated convalescents harbored
271 significantly more spike-specific Tcm and Tn, and less spike-specific Ttm (Fig. 6A). By contrast,
272 Tfh and Treg frequencies were not different between infection-naïve and convalescent
273 vaccinees (Fig. 6B). To broaden our analysis, we assessed for unique features of Cluster A1,
274 which was over-represented in the infection-naïve donors, and Cluster A3, an abundant cluster
275 which was over-represented in the convalescent donors albeit insignificantly (Fig. 5G).
276 Interestingly, Cluster A1 expressed low levels of CD127, CXCR4, and CCR7 in contrast to
277 Cluster A3 (Fig. S4A). As Cluster A1 is enriched among the infection-naïve individuals, these
278 findings suggest that these three receptors may be expressed at lower levels on the cells from
279 these individuals, relative to those from vaccinated convalescents. This was confirmed by our
280 detection of higher expression of CD127, CXCR4, and CCR7 on spike-specific CD4+ T cells
281 from the convalescents, although for CXCR4 the difference did not reach statistical significance
282 (Fig. S4B).
283 We then followed up on each of these three differentially expressed markers. CD127,
284 the alpha chain of the IL7 receptor, can drive IL7-mediated homeostatic proliferation of SARS-
285 CoV-2-specific CD4+ T cells [28], and serves as a marker of long-lived precursor memory cells [35].
286 To assess the potential longevity of the spike-specific CD4+ T cells, we determined the
287 percentage of CD127+ cells expressing low levels of the terminal differentiation marker CD57.
288 After the second dose of vaccination, convalescent individuals harbored more long-lived
289 (CD127+CD57-) spike-specific CD4+ T cells than infection-naïve individuals (Fig. 6C). CXCR4,
290 the second preferentially-expressed marker among the convalescents' spike-specific CD4+ T
291 cells, was recently suggested to direct bystander T cells to the lung during COVID-19, and to be
292 co-expressed with the T resident memory / activation marker CD69 [26]. Interestingly, spike-
293 specific CD4+ T cells from convalescent donors harbored a highly significantly elevated
294 proportion of CXCR4+CD69+ cells (Fig. 6D), suggesting a potentially superior ability to migrate

295 into pulmonary tissues. The last differentially expressed antigen, CCR7, is a chemokine
296 receptor that directs immune cells to lymph nodes. As CD62L, a selectin that also mediates
297 lymph node homing, was also on our panel, we assessed whether CCR7+CD62L+ cells were
298 enriched among the spike-specific CD4+ T cells from the convalescent donors, and found this to
299 be the case (Fig. 6E).

300 Our finding that the convalescent donors' spike-specific CD4+ T cells were preferentially
301 CXCR4+CD69+ and CCR7+CD62L+ suggested that they may preferentially migrate out of the
302 blood into lymphoid tissues. Supporting this possibility was our observation that, after the
303 second vaccine dose, the percentages of CCR7+CD62L+ spike-specific cells increased as the
304 percentages of spike-specific CD4+ T cells decreased (Fig. 6F). This suggests that the low
305 spike-specific CD4+ T cell response after the second dose of vaccination in some convalescent
306 donors (Fig. 1D) may have resulted from these cells preferentially leaving the blood
307 compartment. This was further supported by our finding that the expression levels of CCR7 and
308 CD62L on spike-specific CD4+ T cells inversely correlated with the magnitude of the spike-
309 specific CD4+ T cell response (Fig. 6G). To assess whether the CCR7+CD62L+ and
310 CXCR4+CD69+ CD4+ T cells have the potential to migrate into the nasopharynx, the most
311 common site of SARS-CoV-2 entry, we obtained paired blood and nasal swabs from one of the
312 participants (PID4101) and phenotyped total CD4+ T cells isolated from these specimens.
313 There was a marked enrichment of both CCR7+CD62L+ and CXCR4+CD69+ CD4+ T cells in
314 the intranasal specimens (Fig. 6H), suggesting that CD4+ T cells expressing these markers
315 preferentially exit the blood and enter the nasopharynx. Together, these data suggest that after
316 vaccination, spike-specific CD4+ T cells from convalescent individuals differ from those in
317 infection-naïve individuals in that they appear to be more long-lived, and may more readily
318 migrate out of the blood to mucosal sites, thus explaining their overall lower frequencies
319 measured from the blood.
320

321 **Phenotypic features of spike-specific CD8+ T cells from vaccinated, convalescent**
322 **individuals are unique but differ from their CD4+ T cell counterparts**

323 Finally, we assessed to what extent the main similarities and differences observed with
324 spike-specific CD4+ T cells were also seen for spike-specific CD8+ T cells. Similar to the CD4+
325 T cells, spike-specific CD8+ T cells stimulated by the three different spike proteins (ancestral,
326 B.1.1.7, B.1.351) did not differ in their phenotypic features (Fig. S5A-C). Also similar to the
327 CD4+ T cells, spike-specific CD8+ T cells elicited by vaccination differed phenotypically in the
328 infection-naïve vs. convalescent individuals (Fig. S5D-F). Unlike the CD4+ T cell data, however,
329 these phenotypic differences could not be accounted for by distribution changes among the
330 main canonical subsets Tn, Tscm, Temra, Tcm, Tem, and Ttm (Fig. S5G). Also unlike the CD4+
331 T cells, these differences were also not explained by differential abundance of the
332 CD127+CD57-, CXCR4+CD69+, or CCR7+CD62L+ subsets (Fig. S5H). Instead, the differences
333 appear to be due to other phenotypic changes, including elevated frequencies of activated cells
334 in the convalescent donors, in particular those co-expressing the Tcm marker CD27 and
335 activation marker CD38, and the checkpoint inhibitor molecule CTLA4 and activation marker 4-
336 1BB (Fig. S5I). These results suggest that vaccine-elicited spike-specific CD8+ T cells, like their
337 CD4+ counterparts, respond equivalently to the B.1.1.7 and B.1.351 variants, and exhibit
338 qualitative differences in convalescent individuals but via different phenotypic alterations than
339 their CD4+ counterparts.
340

341 **DISCUSSION**

342 T cells are important orchestrators and effectors during antiviral immunity. They may
343 hold the key to long-term memory due to their ability to persist for decades, yet these cells have
344 been disproportionately understudied relative to their humoral immune counterparts in the
345 context of COVID-19. Here, we designed a longitudinal study assessing both the frequency and
346 phenotypic characteristics of SARS-CoV-2-specific T cells in order to address the following

347 questions: 1) Do SARS-CoV-2-specific T cells elicited by vaccination respond similarly to
348 ancestral and variant strains?, 2) To what extent is the second dose needed for boosting T cell
349 responses in infection-naïve and convalescent individuals?, and 3) Do vaccine-elicited memory
350 T cells differ in infection-naïve vs. convalescent individuals?

351 To answer the first question, we compared post-vaccination SARS-CoV-2 spike-specific
352 T cell responses against ancestral vs. the variant B.1.1.7 and B.1.351 strains. Consistent with
353 recent studies [16-22], we find that vaccination-elicited T cells specific to the ancestral spike protein
354 also recognize variant spike proteins. We further demonstrate that the phenotypic features of
355 these cells are identical, whether they are stimulated by ancestral or variant spike proteins. This
356 was important to establish because of prior reports that effector T cells can respond differently
357 to APLs by altering their cytokine production or by mounting an immunoregulatory response [30,
358 31]. APLs could theoretically arise when a variant infects an individual that was previously
359 exposed to ancestral spike through vaccination or prior infection. That both the quantity and
360 quality of T cell responses is maintained against the variants may provide an explanation for the
361 real-world efficacy of the vaccines against variants. Although limited data are available, thus far
362 all vaccines deployed in areas where the B.1.1.7 or B.1.351 strains dominate have protected
363 vaccinees from severe and fatal COVID-19 [36]. Given the potentially important role of SARS-
364 CoV-2-specific T cells in protecting against severe and fatal COVID-19 [26, 27], we postulate that
365 this protection may have been in large part mediated by vaccine-elicited T cells. In contrast,
366 efficacy of the vaccines against mild or moderate disease in variant-dominated regions of the
367 world is more variable. For example, in South Africa where B.1.351 is dominant, the
368 AstraZeneca ChAdOx1 vaccine only prevented ~10% of mild-to-moderate disease cases [37],
369 while more recent data from Pfizer/BioNTech's vaccine administered in Qatar, where both
370 B.1.1.7 and B.1.351 are dominant, revealed that fully vaccinated individuals were 75% less
371 likely to develop COVID-19 [38]. The overall diminished vaccine-mediated protection against
372 milder disease in variant-dominated regions of the world might be explained by the likely

373 important role of antibodies to prevent initial infection by blocking viral entry into host cells
374 (manifesting as protection against asymptomatic and mildly symptomatic infection), and the
375 observation that vaccine-elicited antibodies are generally less effective against the variant than
376 against ancestral spike in lab assays [6-15]. Reassuringly, there is no evidence that vaccinated
377 individuals mount a weaker immune response to variants than do unvaccinated individuals,
378 which could theoretically result through a phenomenon termed original antigenic sin (where the
379 recall response is inappropriately diverted to the vaccination antigen at the expense of a
380 protective response against the infecting variant strain) [39].
381 To address the second question of whether a booster dose is needed, we compared the
382 T cells after the first vs. second vaccination doses, among the infection-naïve and convalescent
383 individuals. In infection-naïve individuals, spike-specific responses were observed after the first
384 vaccination dose, and were further boosted after the second. This enhancement of the T cell
385 response after the second dose is similar to the reported increase in anti-spike IgG levels after a
386 second dose in infection-naïve individuals [32, 33]. Interestingly, phenotypic changes were also
387 observed after the second dose in that the B cells producing the anti-spike antibodies
388 differentiated from IgM-dominant to IgG-dominant producers [32]. We also observed some
389 phenotypic changes among spike-specific CD4+ T cells after the second dose, as reflected by
390 an increase in the Ttm response at the expense of the Tcm response. Importantly, however,
391 after either dose, spike-specific CD4+ T cells were still primarily Tcm and Tfh cells, the latter of
392 which are important for providing helper function for B cells. The prominence of SARS-CoV-2-
393 specific Tfh cells after just one dose of vaccination is consistent with prior reports that a single
394 dose of SARS-CoV-2 mRNA in mice is sufficient to elicit potent B and Tfh cell responses in
395 germinal centers [40]. These results suggest that with regards to T cells, the booster dose is
396 necessary for enhancing the magnitude and results in some phenotypic changes although a
397 robust Tfh response is already established the first dose. Overall, our conclusions are in line

398 with those drawn from serological studies [32, 33]: that it is important to administer the second
399 vaccine dose in infection-naïve individuals to boost spike-specific responses.
400 A different situation appears to be the case for convalescent individuals. Longitudinal
401 serological studies suggest that the spike-specific antibody response in convalescent individuals
402 after the first mRNA dose is already equivalent to that of infection-naïve individuals after their
403 second mRNA dose [32, 33], suggesting that convalescent individuals may only need a single dose
404 of vaccination. We found no evidence of increased numbers of spike-specific CD4+ T cells after
405 the second dose, and minimal phenotypic changes between the cells at the two post-
406 vaccination timepoints. Spike-specific CD4+ T cells from these individuals did however exhibit
407 marked phenotypic changes as they transitioned from the pre- to the post-vaccination
408 timepoints. This was expected since the cells from the pre-vaccination timepoint are resting
409 memory CD4+ T cells that were primed months prior, while the post-vaccination timepoints were
410 more recently-reactivated memory cells. Interestingly, unlike for the infection-naïve individuals
411 where all individuals responded similarly to each dose of vaccination, the magnitude of the
412 CD4+ T cell response differed markedly between different convalescent individuals. PID4112
413 had a large pool of spike-specific CD4+ T cells prior to vaccination, and their numbers increased
414 to extremely high levels after the first vaccination dose. Surprisingly, this large peak in the spike-
415 specific response was accompanied by an increase in the nucleocapsid-specific CD4+ T cells,
416 which was unexpected since the vaccine does not contain nucleocapsid. We suspect this high
417 response to nucleocapsid was due to inflammation-mediated bystander activation of T cells in
418 an antigen-independent manner. Consistent with this hypothesis, the participant reported severe
419 side effects (severe headache, chills, myalgia, nausea, and diarrhea) after the first dose. The
420 remaining five convalescent donors, by contrast, never exhibited a robust T cell response, and
421 in fact after full vaccination actually exhibited a highly significantly lower CD4+ T cell response
422 than the infection-naïve vaccinees. We speculate on an explanation further below. Overall, our
423 results suggest that a second SARS-CoV-2 vaccine dose in individuals who have recovered

424 from COVID-19 may provide less benefit than in individuals who have not previously been
425 exposed to SARS-CoV-2; these findings are in line with recommendations from previously
426 published serological studies [10, 32, 33].

427 One of the most striking observations from this study, and the third and final question we
428 set out to answer, was the remarkably distinct phenotypes of spike-specific CD4+ T cells from
429 infection-naïve vs. convalescent individuals who were fully vaccinated. The spike-specific CD4+
430 T cells from the convalescent individuals harbored features suggesting increased potential for
431 long-term persistence: they were enriched for Tcm cells, which are have longer *in vivo* half-lives
432 than their Tem and Ttm counterparts [41], and express elevated levels of CD127, a marker of
433 long-lived memory T cells [35]. Interestingly, CD127 expression on SARS-CoV-2-specific T cells
434 has been implicated in COVID-19 disease amelioration and in these cells' long-term
435 persistence. CD127 expression was more frequent on spike-specific CD4+ T cells from ICU
436 patients who eventually survived severe COVID-19 than in those that did not [26]. IL7, the ligand
437 for CD127, can drive homeostatic proliferation and expansion of spike-specific CD4+ T cells [28],
438 and CD127 is not only expressed on SARS-CoV-2-specific memory CD4+ and CD8+ T cells,
439 but its levels increase further over the course of convalescence [28, 42]. Together, these findings
440 suggest that after vaccination, spike-specific CD4+ T cells in convalescent individuals may
441 persist longer than those from infection-naïve individuals, but additional long-term follow-up
442 studies will be required to directly test whether this indeed is the case.

443 Another interesting characteristic of post-vaccination spike-specific CD4+ T cells from
444 convalescent individuals relative to infection-naïve individuals was their expression of multiple
445 tissue-homing receptors. In particular, these cells were preferentially CCR7+CD62L+ and
446 CXCR4+CD69+. CCR7 and CD62L mediate homing to lymph nodes, while CXCR4 is a
447 chemokine receptor important in migration of hematopoietic stem cells to bone marrow, but also
448 able to direct immune cells to the lung during inflammation [43]. Interestingly, we recently
449 observed co-expression of CXCR4 with CD69 (an activation marker that also identifies T

450 resident memory cells) in pulmonary T cells from COVID-19 patients [26]. Many of these cells
451 were bystander (non-SARS-CoV-2-specific) CXCR4+CD69+ T cells whose numbers in blood
452 increased prior to death from COVID-19. We therefore proposed a model whereby recruitment
453 of non-SARS-CoV-2-specific T cells into the lungs of severe patients may exacerbate the
454 cytokine storm and thereby contribute to death [26]. In the case of the vaccinated convalescent
455 individuals, however, expression of CXCR4 and CD69 on SARS-CoV-2-specific T cells is
456 expected to be beneficial as it would direct the T cells capable of recognizing infected cells into
457 the lung. CCR7 and CD62L co-expression would further enable these cells to enter draining
458 lymph nodes and participate in germinal center reactions. Supporting the hypothesis that the
459 post-vaccination spike-specific CD4+ T cells from convalescent individuals may better home to
460 lymphoid tissues is our observation that frequencies of these cells in blood correlated negatively
461 with the extent to which they co-expressed CCR7 and CD62L. This was further supported by
462 our finding that CD4+ T cells from the nasopharynx of the upper respiratory tract were
463 preferentially CCR7+CD62L+ and CXCR4+CD69+ relative to their blood counterparts. All
464 together, these results imply that compared to infection-naïve individuals, convalescents' spike-
465 specific CD4+ T cells may be superior in surviving and migrating to the respiratory tract. Directly
466 testing this hypothesis will require obtaining large numbers of respiratory tract cells from
467 vaccinated, infection-naïve vs. convalescent individuals (e.g., via bronchoalveolar lavages or
468 endotracheal aspirates) for quantitation and characterization of SARS-CoV-2-specific T cells. Of
469 note, vaccination of infection-naïve individuals might not induce a strong humoral immunity in
470 the respiratory mucosa either, as neutralizing antibodies against SARS-CoV-2 are rarely
471 detected in nasal swabs from vaccinees [13]. If it turns out that current vaccination strategies do
472 not ensure robust humoral and cell-mediated immune responses in the respiratory tract, then
473 strategies that better elicit mucosal-homing SARS-CoV-2-specific B and T cells in infection-
474 naïve individuals – for example by implementing an intranasal route of mRNA immunization –
475 may hold a greater chance of achieving sterilizing immunity.

476

477 ***Limitations***

478 As this study was aimed at using in-depth phenotypic characterization as a discovery tool, it
479 focused on deeply interrogating many different conditions (e.g., spike variants, longitudinal
480 sampling) rather than many donors. Therefore, although a total of 165 CyTOF specimens were
481 run, only 11 donors were analyzed. The findings reported here should be confirmed in larger
482 cohorts. A second limitation of the study was the need to stimulate the specimens in order to
483 identify and characterize the vaccine-elicited T cells. We limited peptide exposure to 6 hours to
484 minimize phenotypic changes caused by the stimulation, similar to our prior studies [26, 28]. Finally,
485 the analysis focused on CD4+ T cells because the overall numbers of detectable spike-specific
486 CD8+ T cells were low. Nonetheless, the main findings we made with the CD4+ T cells – that
487 they recognize variants equivalently, and that the phenotypes of the responding cells differ by
488 prior SARS-CoV-2 natural infection status – were recapitulated among CD8+ T cells. Additional
489 studies in a larger number of participants testing more cells, and implementing the use of
490 combinatorial MHC class I tetramers in conjunction with high-parameter phenotyping [44], would
491 increase the ability to characterize in greater depth the vaccine-elicited CD8+ T cell response.

492 **ACKNOWLEDGEMENTS**

493 This work was supported by the Van Auken Private Foundation, David Henke, and Pamela and
494 Edward Taft (N.R.R.); philanthropic funds donated to Gladstone Institutes by The Roddenberry
495 Foundation and individual donors devoted to COVID-19 research (N.R.R.); the Program for
496 Breakthrough Biomedical Research (N.R.R., S.A.L.), which is partly funded by the Sandler
497 Foundation; and Awards #2164 (N.R.R.), #2208 (N.R.R.), and #2160 (to S.A.L.) from Fast
498 Grants, a part of Emergent Ventures at the Mercatus Center, George Mason University. We
499 acknowledge the NIH DRC Center Grant P30 DK063720 and the S10 1S10OD018040-01 for
500 use of the CyTOF instrument. We thank Stanley Tamaki and Claudia Bispo for CyTOF
501 assistance at the Parnassus Flow Core, Heather Hartig for help with recruitment, Françoise
502 Chanut for editorial assistance, and Robin Givens for administrative assistance.

503

504 **AUTHOR CONTRIBUTIONS**

505 J.N. designed and performed experiments, and conducted data analyses; X.L. helped develop
506 an analysis plan and conducted data analyses; M.M. processed and banked specimens; G.X.
507 performed experiments; V.M. conducted CHIRP participant interviews, enrollment, and
508 specimen collection; W.C.G. participated in data analysis, performed supervision, and edited the
509 manuscript; S.A.L. established the CHIRP cohort, conducted CHIRP participant interviews,
510 enrollment, and specimen collection, and edited the manuscript; N.R.R. conceived ideas for the
511 study, performed supervision, conducted data analyses, and wrote the manuscript. All authors
512 read and approved the manuscript.

513

514 **COMPETING FINANCIAL INTERESTS:** The authors declare no competing financial interests.

515 **METHODS**

516

517 ***Human Subjects***

518 Eleven participants from the COVID-19 Host Immune Pathogenesis (CHIRP) cohort were
519 recruited for this study. Six were previously infected with SARS-CoV-2 as established by RT-
520 PCR, and had fully recovered from a mild course of disease. Importantly, infections of these six
521 individuals had all occurred in the San Francisco Bay Area between March – July of 2020, when
522 the dominant local strain was the original ancestral (Wuhan) strain. The remaining five
523 participants were not previously infected with the virus. All eleven participants were vaccinated
524 with both doses of either of the Moderna or Pfizer/BioNTech mRNA vaccines (Table S1). Blood
525 was drawn from each of the eleven participants prior to vaccination, ~2 weeks after the first
526 vaccine dose, and ~2 weeks after the second vaccine dose (33 specimens total). On the day of
527 each blood draw, PBMCs were isolated from blood using Lymphoprep™ (StemCell
528 Technologies), and then cryopreserved in 90% fetal bovine serum (FBS) and 10% DMSO. For
529 participant PID4101, an additional blood-draw and intranasal swab specimens were obtained for
530 immunophenotyping studies. This study was approved by the University of California, San
531 Francisco (IRB # 20-30588).

532

533 ***Preparation of specimens for CyTOF***

534 Cryopreserved PBMCs were revived and cultured overnight to allow for antigen
535 recovery. The cells were then counted, and then two million cells per treatment condition were
536 stimulated with the co-stimulatory agents 0.5 μg/ml anti-CD49d clone L25 and 0.5 μg/ml anti-
537 CD28 clone L293 (both from BD Biosciences), in the presence of 0.5 μM of overlapping 15-mer
538 SARS-CoV-2 spike peptides PepMix™ SARS-CoV-2 peptides from the original SARS-CoV-2
539 strain, B.1.1.7, or B.1.351, or overlapping 15-mer SARS-CoV-2 nucleocapsid peptides (all from
540 JPT Peptide Technologies). Stimulations were conducted for 6 hours in RP10 media (RPMI

541 1640 medium (Corning) supplemented with 10% FBS (VWR), 1% penicillin (Gibco), and 1%
542 streptomycin (Gibco)), in the presence of 3 μg/ml Brefeldin A Solution (eBioscience) to enable
543 detection of intracellular cytokines. To establish the phenotypes of total T cells in the absence of
544 stimulation, two million cells were cultured in parallel with the stimulated samples, but in the
545 presence of only 3 μg/ml Brefeldin A.

546 After culture, the cells were treated with cisplatin (Sigma-Aldrich) as a live/dead marker
547 and fixed with paraformaldehyde (PFA) as previously described [28, 45]. Cisplatin treatment and
548 fixation was performed as follows: first, cells were resuspended in 2 ml PBS (Rockland) with 2
549 ml EDTA (Corning), followed by addition of 2 ml PBS/EDTA supplemented with 25 μM cisplatin
550 (Sigma-Aldrich) for 60 seconds. Cisplatin staining was then quenched with 10 ml of CyFACS
551 (metal contaminant-free PBS (Rockland) supplemented with 0.1% FBS and 0.1% sodium azide
552 (Sigma-Aldrich)), centrifuged, and resuspended in 2% PFA in CyFACS. Fixation was allowed to
553 proceed for 10 minutes at room temperature, after which cells were washed twice with CyFACS,
554 and then resuspended in CyFACS containing 10% DMSO. Fixed cells were stored at -80°C until
555 analysis by CyTOF. For paired blood/swab specimens from PID4101, cells were immediately
556 cisplatin-treated and fixed, without prior cryopreservation.

557

558 ***CyTOF staining and data acquisition***

559 CyTOF staining was conducted in a fashion similar to recently described methods [26, 28,
560 45-48]. Cisplatin-treated cells were thawed, counted, and each treatment condition was barcoded
561 using the Cell-ID 20-Plex Pd Barcoding Kit (Fluidigm). After the cells were barcoded and
562 washed, the barcoded samples were combined and diluted to 6 x 10^6 cells / 800 μl CyFACS per
563 well in Nunc 96 DeepWell™ polystyrene plates (Thermo Fisher). Cells were blocked with mouse
564 (Thermo Fisher), rat (Thermo Fisher), and human AB (Sigma-Aldrich) sera for 15 minutes at
565 4°C, and then washed twice in CyFACS. Surface CyTOF antibody staining (Table S2) was

566 conducted for 45 minutes at 4°C, in a volume of 100 μl / sample. Cells were then washed three
567 times with CyFACS and fixed overnight at 4°C in 100 μl of 2% PFA in PBS. The next day,
568 samples were washed twice with Intracellular Fixation & Permeabilization Buffer (eBioscience),
569 and incubated for 45 minutes at 4°C. After two additional washes with Permeabilization Buffer
570 (eBioscience), samples were blocked for 15 minutes at 4°C in 100 μl of Permeabilization Buffer
571 containing mouse and rat sera. After one additional wash with Permeabilization Buffer, samples
572 were stained with the intracellular CyTOF antibodies (Table S2) at 4°C for 45 minutes in a
573 volume of 100 μl / sample. Cells were then washed once with CyFACS, and stained for 20
574 minutes at room temperature with 250 nM of Cell-ID™ Intercalator-IR (Fluidigm). Immediately
575 prior to sample acquisition, cells were washed twice with CyFACS buffer, once with MaxPar®
576 cell staining buffer (Fluidigm), and once with Cell acquisition solution (CAS, Fluidigm). Cells
577 were resuspended in EQ™ Four Element Calibration Beads (Fluidigm) diluted in CAS
578 immediately prior to acquisition on a Helios-upgraded CyTOF2 instrument (Fluidigm) at the
579 UCSF Parnassus flow core facility.
580
581 ***CyTOF data analysis***
582 CyTOF datasets, exported as flow cytometry standard (FCS) files, were de-barcoded
583 and normalized according to manufacturer's instructions (Fluidigm). FlowJo software (BD
584 Biosciences) was used to identify CD4+ T cells (live, singlet CD3+CD19-CD4+CD8-) and CD8+
585 T cells (live, singlet CD3+CD19-CD4-CD8+) among all analyzed samples. IFNγ+ in the
586 stimulated samples were considered to be the SARS-CoV-2-responsive cells. For high-
587 dimensional analyses of SARS-CoV-2-specific T cells among the stimulated samples, we
588 excluded samples with an insufficient number of events (≤ 3) to limit skewing of the data.
589 Manual gating analysis was initially performed using FlowJo, and then select populations were
590 exported as FCS files and then imported into R software as GatingSet objects. Using the

591 *CytoExploreR* package, 2D-gates were manually drawn on the imported samples. The 2D dot
592 plots and statistical results were exported for data visualization, bar-graph generation, and
593 statistical comparisons as previously described
594 (https://github.com/DillonHammill/CytoExploreR). High-dimensional analyses (MDS, tSNE, and
595 flowSOM) were performed using R software by implementing a CyTOF workflow recently
596 described [49].

597 For MDS plot generation, we used the plotMDS function from the *limma* package with
598 default settings. Euclidean distances between all samples were calculated using the arcsinh-
599 transformed median expression levels with cofactor 5, of the lineage and functional markers
600 listed below.

CD8	Lineage (Only for CD8 subset)
CD4	Lineage (Only for CD4 subset)
CD161	Lineage
HLADR	Lineage
CD45RO	Lineage
CD69	Lineage
CRTH2	Lineage
PD1	Lineage
CXCR5	Lineage
CD27	Lineage
CD3	Lineage
CD2	Lineage
CD62L	Lineage
CCR6	Lineage
OX40	Lineage
CD28	Lineage
CD127	Lineage
RORγt	Lineage
CXCR4	Lineage
CTLA4	Lineage
NFAT	Lineage
CCR5	Lineage
CD137	Lineage
CD95	Lineage
ICOS	Lineage
CD49d	Lineage
CD7	Lineage
Tbet	Lineage
TIGIT	Lineage

CCR7	Lineage
CD45RA	Lineage
CD57	Lineage
CD38	Lineage
$\alpha 4\beta 7$	Lineage
CD25	Lineage
IFNγ	Function
IL6	Function
IL4	Function
IL17	Function

601

602 The first (MDS1) and second (MDS2) MDS dimensions were plotted to show the dissimilarities
603 between samples from the indicated conditions as described [34].

604 tSNE was performed using the Trsne function from the *Rtsne* package using arcsinh-
605 transformed expression of lineage markers (no PCA step, iterations = 1000, perplexity = 30,
606 theta = 0.5). Events corresponding to unstimulated T cells were down-sampled to 1000 cells per
607 sample, and SARS-CoV-2-specific cells (cell numbers ranging from 4 to 229 per sample) were
608 all included in the tSNE analyses without down-sampling. Each cell was displayed in a tSNE
609 plot for dimension reduction visualization and colored with arcsinh-transformed cell marker
610 expression as heatmaps, or pseudo-colored by the appropriate group.

611 Unsupervised cell subset clustering was performed using FlowSOM [50] and
612 *ConsensusClusterPlus* packages using arcsinh-transformed expression levels of the lineage
613 markers indicated above [51]. For clustering of SARS-CoV-2-specific T cells, we set the meta-
614 cluster number to 8 and cluster number to 40. The frequency of each cluster within each sample
615 was calculated using the following equation:

616

617 (Frequency of cluster in specified sample) = (Cell count of cluster / Total cell count of specified
618 sample)

619

620 This was then converted to a percentage by multiplying by 100. The percentages of each cluster
621 from the selected samples were plotted as box plots with jittered points, followed by statistical
622 analysis between the groups. To compare the abundance distribution of clusters between
623 groups, frequencies of clusters in samples from each group were normalized using the equation
624 below:
625
626 (Normalized frequency of cluster in specified sample) = (Frequency of cluster in specified
627 sample/ Total number of samples in each group)
628
629 This was then converted to a percentage by multiplying by 100, and plotted as stacked bar
630 charts.
631
632 ***Statistical Analysis***
633 The statistical tests used in comparison of groups are indicated within the figure legends. For 2-
634 group comparisons, student's t-tests were performed and p-values were adjusted for multiple
635 testing using the Holm-Sidak method where applicable. For comparisons of 3 or more groups,
636 significance between groups was first evaluated by one-way ANOVA, and then the p-values
637 were adjusted for multiple testing using the Holm-Sidak method where applicable. For datasets
638 with significant ANOVA-adjusted p-values (≤ 0.05), we performed Tukey's honestly significant
639 difference (HSD) post-hoc test to determine the p-values between individual groups.
640
641 ***Raw Data Availability***
642 For this study, a total of 120 specimens were analyzed by CyTOF. Each specimen included
643 both CD4+ and CD8+ T cells. For each specimen, we gated separately on events
644 corresponding to CD4+ T cells (live, singlet CD3+CD4+CD8-) and CD8+ T cells (live, singlet

645 CD3+CD4-CD8+), and exported the files as 240 individual FCS files. These 240 raw CyTOF
646 datasets are available for download through the public repository Dryad via the following link:
647 https://doi.org/10.7272/Q60R9MMK

648 **MAIN FIGURE LEGENDS**

649

650 **Figure 1. SARS-CoV-2-specific T cells elicited by vaccination recognize variants, and in a**
651 **manner that differs among individuals with prior COVID-19.** (**A**) Identification of vaccine-
652 elicited spike-specific T cells. PBMCs before vaccination (Pre-Vac) or 2 weeks after each dose
653 of vaccination were stimulated with spike peptides and assessed by CyTOF 6 hours later for the
654 presence of spike-specific (IFNγ-producing) CD4+ (*left*) or CD8+ (*right*) T cells. The "no peptide"
655 conditions served as negative controls. Shown are longitudinal data from an infection-naïve
656 (PID4101, *top*) and convalescent (PID4112, *bottom*) individual. **(B)** Quantification of the spike-
657 specific CD4+ (*left*) and CD8+ (*right*) T cells recognizing the ancestral (squares), B.1.1.7
658 (triangles), and B.1.351 (circles) spike peptides in infection-naïve (*top*) and convalescent
659 (*bottom*) individuals before and after vaccination. Note the similar frequencies of T cells
660 responding to all three spike proteins in each donor, the clear boosting of spike-specific CD4+ T
661 cell frequencies in infection-naïve but not convalescent individuals, and the overall higher
662 proportion of responding CD4+ than CD8+ T cells. The dotted line corresponds to the
663 magnitude of the maximal pre-vaccination response in infection-naïve individuals and is
664 considered as background. The y-axes are fitted based upon the maximal post-vaccination
665 response values for each patient group and T cell subset. The *p*-values shown (**$p < 0.01$, ***p
666 < 0.001) were calculated by student's t-test. **(C)** As expected, nucleocapsid-specific T cell
667 responses are generally low over the course of vaccination, with the exception of convalescent
668 donor PID4112. Shown are the frequencies of nucleocapsid-specific CD4+ (*left*) and CD8+
669 (*right*) T cells, as measured by IFNγ production upon stimulation with ancestral nucleocapsid
670 peptides, in infection-naïve (*top*) and convalescent (*bottom*) individuals. The dotted line
671 corresponds to the magnitude of the maximal pre-vaccination response infection-naïve
672 individuals, and is considered as the background signal. Y-axes are labeled to match the

673 corresponding y-axes for spike-specific T cell responses in *panel B*. **(D)** The CD4+ T cell
674 response is boosted by the second vaccine dose to a greater extent in infection-naïve than
675 convalescents individuals. Shown are the frequencies of spike-specific CD4+ (*left*) and CD8+
676 (*right*) T cells stimulated by the three spike proteins (squares: ancestral; triangles: B.1.1.7;
677 circles: B.1.351) among the infection-naïve (aqua) and convalescent (coral) donors, after
678 removal of outlier PID4112. ***$p < 0.001$ comparing the infection-naïve vs. convalescent post-
679 dose 2 specimens, were calculated using student's t-test.
680
681 **Figure 2. SARS-CoV-2-specific CD4+ T cells responding to B.1.1.7 and B.1.351 spike have**
682 **the same phenotypes as those responding to ancestral spike. (A)** Datasets corresponding
683 to spike-specific CD4+ T cells after vaccination were visualized as a multidimensional scaling
684 (MDS) plot. Each datapoint reflects the cumulative phenotypes averaged across all the SARS-
685 CoV-2-specific CD4+ T cells from a single stimulated sample. Data for both infection-naïve and
686 convalescent individuals, and for both the post-dose 1 and post-dose 2 timepoints, are shown.
687 The lack of segregation of the cells responding to the ancestral, B.1.1.7, and B.1.351 spike
688 proteins suggest phenotypic similarities. **(B)** Visualization of the datasets by tSNE dot plots.
689 CD4+ T cells responding to ancestral or variant spike stimulation by producing high amounts of
690 IFNγ (*right*) segregate together and away from the total CD4+ T cell population (*left*). Each dot
691 represents one cell. **(C)** CD4+ T cells responding to ancestral spike and its variants are
692 phenotypically similar, as shown by their complete mingling on a tSNE dot plot. **(D, E)** Spike-
693 responding CD4+ T cells are mostly memory cells, as indicated by high CD45RO and low
694 CD45RA expression levels, and include those expressing high levels of Tcm, Tfh, activation,
695 and respiratory tract migration markers. Shown is the tSNE depicted in *panel C* displaying the
696 relative expression levels of the indicated antigens (Red: high; Blue: low). **(F)** CD4+ T cells
697 responding to ancestral spike and its variants distribute in a similar fashion among the 8 clusters
698 identified by flowSOM. Shown on the left is the distribution of T cells responding to ancestral or

699 variant spike peptides on the tSNE depicted in *panel C,* colored according to the flowSOM
700 clustering. Shown on the right is the quantification of the flowSOM distribution data. No
701 significant differences were observed between the three groups in the distribution of their cells
702 among the 8 clusters, as calculated using a one-way ANOVA and adjusted for multiple testing
703 (n = 8) using Holm-Sidak method ($p > 0.05$).
704
705 **Figure 3. Phenotypes of spike-specific CD4+ T cells from infection-naïve individuals**
706 **following first and second dose of vaccination. (A)** MDS plot depicting samples of spike-
707 specific CD4+ T cells in vaccinated infection-naïve individuals, showing some interspersion of
708 the cells from the two post-vaccination timepoints. Each dot represents a single specimen. **(B)**
709 tSNE dot plot of spike-specific CD4+ T cells from vaccinated infection-naïve individuals. Each
710 dot represents a single cell. **(C)** tSNE plots depicting cells from the two timepoints, colored
711 according to the cells' cluster classification as determined by flowSOM. **(D)** Distribution among
712 flowSOM clusters of post-vaccination spike-specific CD4+ T cells from infection-naïve
713 individuals between the two post-vaccination timepoints. **(E)** Two clusters of spike-specific
714 CD4+ T cells (B5 and B8) are differentially abundant after the first vs. second vaccination
715 doses. *$p < 0.05$, *** $p < 0.001$ as determined using student's t-tests adjusted for multiple testing
716 (n = 8) using Holm-Sidak method. **(F)** The Tcm markers CD27 and CCR7 are differentially
717 expressed among Clusters B5 and B8, as depicted by histograms. **(G)** The proportions of Tn
718 (CD45RO-CD45RA+CCR7+CD95-), Tscm (CD45RO-CD45RA+CCR7+CD95+), Temra
719 (CD45RO-CD45RA+CCR7-), Tcm (CD45RO+CD45RA-CCR7+CD27+), Tem
720 (CD45RO+CD45RA-CCR7-CD27-), and Ttm (CD45RO+CD45RA-CCR7-CD27+) among spike-
721 specific CD4+ cells in infection-naive individuals after the first vs. second vaccination doses. *p
722 < 0.05, ***$p < 0.001$, ns = non-significant as determined by student's t-test. **(H)** The proportions
723 of Tfh (CD45RO+CD45RA-PD1+CXCR5+) and Treg (CD45RO+CD45RA-CD25+CD127^{low})

724 among spike-specific CD4+ T cells are similar in infection-naive individuals after the first vs.
725 second vaccination doses. ns = non-significant as determined by student's t-test.
726
727 **Figure 4. Differentiation of spike-specific memory CD4+ T cells after vaccination of**
728 **convalescent individuals. (A)** MDS plot depicting datasets corresponding to spike-specific
729 CD4+ T cells in convalescent individuals before and after vaccination. **(B)** tSNE contour
730 heatmaps of spike-specific CD4+ T cells from convalescent individuals emphasizes phenotypic
731 differences between the pre- and post-vaccination cells. Cell densities are represented by color.
732 **(C)** tSNE dot plot of spike-specific CD4+ T cells from convalescent individuals, demonstrating
733 the distinct localization of the pre-vaccination cells on the right. **(D)** Spike-specific CD4+ T cells
734 are phenotypically distinct between the pre- and post-vaccination specimens. Shown are tSNE
735 plots depicting cells from the three indicated timepoints, colored according to the cells' cluster
736 classification as determined by flowSOM. **(E)** The distribution of spike-specific CD4+ T cells
737 classified as flowSOM clusters differs between the pre- and post-vaccination timepoints. **(F)**
738 Multiple clusters of spike-specific CD4+ T cells are differentially abundant between the pre- and
739 post-vaccination specimens. **$p < 0.01$, ***$p < 0.001$, ****$p < 0.0001$ as determined by one-way
740 ANOVA and adjusted for multiple testing ($n = 8$) using the Holm-Sidak method followed by
741 Tukey's honestly significant difference (HSD) post-hoc test. **(G)** Spike-specific CD4+ Tcm
742 increase in convalescent individuals after vaccination. Shown are the proportions of Tn, Tscm,
743 Temra Tcm, Tem, and Ttm among spike-specific CD4+ cells in convalescent individuals before
744 and after vaccination. **(H)** Spike-specific CD4+ Tfh increase in convalescent individuals after
745 vaccination. Shown are the proportions of Tfh and Treg among spike-specific CD4+ T cells in
746 convalescent individuals before and after vaccination. **(I)** Spike-specific CD4+ T cells expressing
747 ICOS and Ox40 increase in convalescent individuals after vaccination. In panels *G-I*, *$p < 0.05$,
748 **$p < 0.01$, ***$p < 0.001$, and ****$p < 0.0001$ as determined by one-way ANOVA followed by
749 Tukey's HSD post-hoc test.

750

751 **Figure 5. Phenotypic features of spike-specific CD4+ T cells differ between infection-**
752 **naïve and convalescent individuals after vaccination. (A)** The frequency of spike-specific
753 CD4+ T cells is similar in infection-naïve and convalescent individuals two weeks after the
754 second vaccination dose. Note that when convalescent donor PID4112, who had an unusually
755 high pre-vaccination frequency of spike-specific CD4+ T cells (Fig. 1D), was excluded, the
756 frequency was significantly lower among the convalescents. **(B)** MDS plots of the phenotypes of
757 spike-specific CD4+ T cells in infection-naïve and convalescent individuals after first and second
758 dose vaccinations. **(C)** tSNE contour heatmaps of spike-specific CD4+ T cells from infection-
759 naïve and convalescent individuals, after first and second dose vaccinations, highlighting the
760 phenotypic differences between the two groups of patients. Cell densities are represented by
761 color. **(D)** tSNE dot plot of spike-specific CD4+ T cells from infection-naïve and convalescent
762 individuals after second dose of vaccination, demonstrating the segregation of the cells from the
763 two groups of patients. **(E)** Spike-specific CD4+ T cells are phenotypically distinct between the
764 infection-naïve and convalescent individuals. Shown are tSNE plots depicting cells after the
765 second dose of vaccination, colored according to the cells' cluster classification as determined
766 by flowSOM. **(F)** The distribution of spike-specific CD4+ T cells into flowSOM clusters differs
767 between the infection-naïve and convalescent individuals after the second vaccine dose. **(G)**
768 Cluster A1 is over-represented in infection-naïve relative to convalescent individuals after the
769 second dose of vaccination. **$p < 0.01$, as determined by student's t-tests adjusted for multiple
770 testing ($n = 8$) using the Holm-Sidak method.

771

772 **Figure 6. The post-vaccination spike-specific CD4+ T cells of convalescents harbor**
773 **phenotypic features of elevated longevity and tissue homing. (A)** Spike-specific CD4+ T
774 cells from convalescent vaccinated individuals harbor higher proportions of Tn and Tcm cells
775 and lower proportions of Ttm cells than those from infection-naïve vaccinated individuals. The

776 proportions of Tn, Tscm, Temra, Tcm, Tem, and Ttm cells among spike-specific CD4+ T cells
777 were determined by manual gating. **p < 0.01, ***p < 0.001, ****p < 0.0001, ns = non-
778 significant, as determined by student's t-test. **(B)** The proportions of Tfh and Treg among spike-
779 specific CD4+ T cells are similar in infection-naïve vs. convalescent individuals after
780 vaccination. ns = non-significant, as determined by student's t-test. **(C)** Spike-specific CD4+ T
781 cells expressing the homeostatic proliferation marker CD127 and lacking expression of the
782 terminal differentiation marker CD57 are more frequent in vaccinated convalescent than
783 vaccinated infection-naïve individuals. **p < 0.01, as determined by student's t-test. **(D)** Spike-
784 specific CD4+ T cells expressing CXCR4, which directs cells to tissues including the lung, and
785 CD69, a marker of T cell activation and tissue residence, are more frequent in convalescent
786 vaccinated individuals. ***p < 0.001, as determined by student's t-test. **(E)** Spike-specific CD4+
787 T cells expressing the lymph node homing receptors CCR7 and CD62L are more frequent in
788 vaccinated convalescent individuals. *p < 0.05, as determined by student's t-test. **(F)** The
789 proportions of CCR7+CD62L+ cells among spike-specific CD4+ T cells associate negatively
790 with the frequencies of spike-specific CD4+ T cells after the second dose of vaccination
791 (correlation coefficient (R) < 0). *P*-values were calculated using t distribution with n-2 degrees
792 of freedom. **(G)** Expression levels (reported as mean signal intensity, or MSI) of CCR7 and
793 CD62L among spike-specific CD4+ T cells associate negatively (R < 0) with overall frequencies
794 of spike-specific CD4+ T cells after the second dose of vaccination. *P*-values were calculated
795 using t distribution with n-2 degrees of freedom. The 95% confidence intervals of the regression
796 lines in the scatter plots of *panels F-G* are shaded in grey. **(H)** CCR7+CD62L+ and
797 CXCR4+CD69+ CD4+ T cells are more frequent in nasopharynx than blood. Unstimulated
798 CD4+ T cells from the blood (*grey*) or from an intranasal swab (*red*) were obtained on the same
799 day from PID4101 and then phenotyped by CyTOF. Numbers indicate the percentages of the
800 corresponding cell population within the gate. Results are gated on live, singlet CD3+CD4+CD8-
801 cells.

802

803 **SUPPLEMENTARY FIGURE LEGENDS**

804

805 **Figure S1. Six-hour stimulation with spike peptides does not induce significant**
806 **expression of activation markers in SARS-CoV-2-specific T cells. (A)** CD4+ T cells were
807 assessed for co-expression of the activation-induced markers (AIM) Ox40 and 4-1BB following
808 6 hours of stimulation with ancestral spike peptides using PBMC specimens from a
809 representative infection-naïve individual (PID4197) before vaccination (Pre-Vac), or two weeks
810 after dose 1 or dose 2 of vaccination. **(B)** CD8+ T cells were assessed for co-expression of the
811 AIM CD69 and 4-1BB following 6 hours of stimulation, using same specimens as *panel A*.
812 Baseline specimens not treated with peptide are shown as a comparison control. Numbers
813 correspond to percentages of cells within the gates. Note that the activated (AIM+) cells that
814 appear in stimulated specimens probably do not reflect peptide-specific stimulation as AIM+
815 cells are also detected in the baseline specimens.

816

817 **Figure S2. Expression levels of all CyTOF phenotyping markers are equivalent between**
818 **CD4+ T cells responding to stimulation by spike from ancestral, B.1.1.7, and B.1.351**
819 **spike.** Shown are the mean expression levels of each antigen in post-vaccination spike-
820 responding CD4+ T cells quantitated by CyTOF. Each datapoint corresponds to a single
821 specimen. No significant differences were observed in expression levels for any of the antigens
822 between any of the three groups, as assessed by one-way and ANOVA adjusted for multiple
823 testing (n = 39) using the Holm-Sidak method ($p > 0.05$).

824

825 **Figure S3. Antigens differentially expressed among Clusters C2 and C5, differentially**
826 **represented among pre- vs. post-vaccination spike-specific CD4+ T cells from**
827 **convalescent individuals.** Shown are histogram depictions of the expression levels of the

828 indicated activation markers in Cluster C2 **(A)** or C5 **(B)** from convalescent individuals. Cluster
829 C2 was more abundant post-vaccination, while Cluster C5 was more abundant pre-vaccination.
830
831 **Figure S4. Cluster A1, enriched among spike-specific CD4+ T cells from infection-naïve**
832 **relative to convalescent vaccinees, express low levels of markers of homeostatic**
833 **proliferation and tissue homing. (A)** Shown are histograms of the expression levels of the
834 alpha chain of the IL7 receptor (CD127), the chemokine receptor CXCR4, and the lymph node
835 homing receptor CCR7, among clusters A1 or A3, the former of was enriched in infection-naïve
836 relative to convalescent individuals after vaccination. Data were concatenated from all clustered
837 cells. **(B)** Relative expression levels, as depicted by normalized mean signal intensity (MSI), of
838 CD127, CXCR4, and CCR7 among all specimens of spike-specific CD4+ T cells from infection-
839 naïve and convalescent individuals, after the second vaccination dose. *$p < 0.05$, **$p < 0.01$, ns
840 = non-significant, as determined using student's t-tests and corrected for multiple testing (n =
841 39) using the Holm-Sidak method.
842
843 **Figure S5. Phenotypic features of spike-specific CD8+ T cells from vaccinated,**
844 **convalescent individuals are unique and differ from those of their CD4+ T cell**
845 **counterparts. (A-C)** MDS (*A*) or tSNE (*B, C*) plots demonstrating phenotypic similarities
846 between spike-specific CD8+ T cells responding to spike from the ancestral, B.1.1.7, or B.1.351
847 strains. Data are displayed in a format similar to that for CD4+ T cells presented in Fig. 2A-C.
848 **(D)** MDS plot depicting specimens of spike-specific CD8+ T cells in infection-naïve and
849 convalescent individuals after second vaccination dose. **(E)** tSNE contour heatmaps depicting
850 spike-specific CD8+ T cells from infection-naïve and convalescent individuals, after the second
851 vaccination dose. Cell densities are represented by color. **(F)** tSNE dot plot of spike-specific
852 CD8+ T cells from infection-naïve and convalescent individuals after second vaccination dose.
853 **(G)** The distribution of spike-specific cells among the main canonical CD8+ T cell subsets (Tn,

854 Tscm, Temra, Tcm, Tem, Ttm) is similar in infection-naïve vs. convalescent individuals after
855 second vaccination dose. **(H)** T cell subsets that were differentially enriched in infection-naïve
856 vs. convalescent individuals among spike-specific CD4+ T cells after second vaccination dose
857 (Fig. 6C) are not differentially enriched among spike-specific CD8+ T cells. Shown are the
858 proportions of cells that are CD127+CD57-, CXCR4+CD69+, or CCR7+CD62L+ cells among
859 spike-specific CD8+ T cells as determined by manual gating. **(I)** Cells co-expressing CD27 and
860 CD38, and CTLA4 and CD137, are elevated among spike-specific CD8+ T cells from
861 vaccinated convalescent individuals relative to vaccinated infection-naïve individuals. *$p < 0.05$,
862 **$p < 0.01$ as determined by student's t-test.

863 **SUPPLEMENTARY TABLES**

864

865 **Table S1. Participant Characteristics**

Patient ID	Gender	Age	Prior Infection Status	Vaccine	Days post PCR+ test at pre-vaccination timepoint	Days post vaccine dose #1	Days post vaccine dose #2
PID4101	Female	45	Uninfected	Pfizer/BioNT	NA	13	12
PID4109	Male	33	Uninfected	Pfizer/BioNT	NA	12	33
PID4197	Female	76	Uninfected	Pfizer/BioNT	NA	14	13
PID4198	Male	79	Uninfected	Moderna	NA	18	10
PID4199	Female	32	Uninfected	Pfizer/BioNT	NA	14	10
PID4104	Female	33	Convalescent	Moderna	212	14	14
PID4108	Female	20	Convalescent	Pfizer/BioNT	226	13	38
PID4112	Female	59	Convalescent	Moderna	254	16	13
PID4114	Female	46	Convalescent	Moderna	216	16	50
PID4117	Female	51	Convalescent	Pfizer/BioNT	82	16	6
PID4118	Female	39	Convalescent	Pfizer/BioNT	173	18	28

866

867 **Table S2. List of CyTOF antibodies used in study**. Antibodies were either purchased from
868 the indicated vendor or prepared in-house using commercially available MaxPAR conjugation
869 kits per manufacturer's instructions (Fluidigm).
870

Antigen Target	Clone	Elemental Isotope	Vendor
HLADR	TÜ36	Qdot (112Cd)	Thermofisher
RORγt*	AFKJS-9	115 In	In-house
CD49d (α4)	9F10	141Pr	Fluidigm
CTLA4*	14D3	142Nd	In-house
NFAT*	D43B1	143Nd	Fluidigm
CCR5	NP6G4	144Nd	Fluidigm
CD137	4B4-1	145Nd	In-house
CD95	BX2	146Nd	In-house
CD7	CD76B7	147Sm	Fluidigm
ICOS	C398.4A	148Nd	Fluidigm
Tbet*	4B10	149Sm	In-house
IL4*	MP4-25D2	150Nd	In-house
CD2	TS1/8	151Eu	Fluidigm
IL17*	BL168	152Sm	In-house
CD62L	DREG56	153Eu	Fluidigm
TIGIT	MBSA43	154Sm	Fluidigm
CCR6	11A9	155Gd	In-house
IL6*	MQ2-13A5	156 Gd	In-house
CD8	RPA-T8	157Gd	In-house
CD19	HIB19	157Gd	In-house
CD14	M5E2	157Gd	In-house
OX40	ACT35	158Gd	Fluidigm
CCR7	G043H7	159Tb	Fluidigm
CD28	CD28.2	160Gd	Fluidigm
CD45RO	UCHL1	161Dy	In-house
CD69	FN50	162Dy	Fluidigm
CRTH2	BM16	163Dy	Fluidigm
PD-1	EH12.1	164Dy	In-house
CD127	A019D5	165Ho	Fluidigm
CXCR5	RF8B2	166Er	In-house
CD27	L128	167Er	Fluidigm
IFNγ*	B27	168Er	Fluidigm
CD45RA	HI100	169Tm	Fluidigm
CD3	UCHT1	170Er	Fluidigm
CD57	HNK-1	171Yb	In-house
CD38	HIT2	172Yb	Fluidigm
α4β7	Act1	173Yb	In-house
CD4	SK3	174Yb	Fluidigm
CXCR4	12G5	175Lu	Fluidigm
CD25	M-A251	176Yb	In-house
CD161	NKR-P1A	209 Bi	In-house

871 *Intracellular antibodies
872

873 **REFERENCES**

874 1. Korber B, Fischer WM, Gnanakaran S, Yoon H, Theiler J, Abfalterer W, Hengartner N,
875 Giorgi EE, Bhattacharya T, Foley B, et al. (2020). Tracking Changes in SARS-CoV-2 Spike:
876 Evidence that D614G Increases Infectivity of the COVID-19 Virus. Cell 182, 812-827 e819.
877 2020/07/23.

878 2. Weissman D, Alameh MG, de Silva T, Collini P, Hornsby H, Brown R, LaBranche CC,
879 Edwards RJ, Sutherland L, Santra S, et al. (2021). D614G Spike Mutation Increases SARS CoV-
880 2 Susceptibility to Neutralization. Cell Host Microbe 29, 23-31 e24. 2020/12/12.

881 3. Plante JA, Mitchell BM, Plante KS, Debbink K, Weaver SC and Menachery VD. (2021).
882 The variant gambit: COVID-19's next move. Cell Host Microbe 29, 508-515. 2021/04/01.

883 4. Callaway E. (2021). Delta coronavirus variant: scientists brace for impact. Nature 595, 17-
884 18. 2021/06/24.

885 5. Davies NG, Jarvis CI, Group CC-W, Edmunds WJ, Jewell NP, Diaz-Ordaz K and Keogh
886 RH. (2021). Increased mortality in community-tested cases of SARS-CoV-2 lineage B.1.1.7.
887 Nature. 2021/03/17.

888 6. Wang P, Nair MS, Liu L, Iketani S, Luo Y, Guo Y, Wang M, Yu J, Zhang B, Kwong PD, et
889 al. (2021). Antibody Resistance of SARS-CoV-2 Variants B.1.351 and B.1.1.7. Nature.
890 2021/03/09.

891 7. Collier DA, De Marco A, Ferreira I, Meng B, Datir R, Walls AC, Kemp SS, Bassi J, Pinto
892 D, Fregni CS, et al. (2021). Sensitivity of SARS-CoV-2 B.1.1.7 to mRNA vaccine-elicited
893 antibodies. Nature. 2021/03/12.

894 8. Muik A, Wallisch AK, Sanger B, Swanson KA, Muhl J, Chen W, Cai H, Maurus D, Sarkar
895 R, Tureci O, et al. (2021). Neutralization of SARS-CoV-2 lineage B.1.1.7 pseudovirus by
896 BNT162b2 vaccine-elicited human sera. Science 371, 1152-1153. 2021/01/31.

897 9. Garcia-Beltran WF, Lam EC, St Denis K, Nitido AD, Garcia ZH, Hauser BM, Feldman J,
898 Pavlovic MN, Gregory DJ, Poznansky MC, et al. (2021). Multiple SARS-CoV-2 variants escape
899 neutralization by vaccine-induced humoral immunity. Cell. 2021/03/21.
900 10. Stamatatos L, Czartoski J, Wan YH, Homad LJ, Rubin V, Glantz H, Neradilek M, Seydoux
901 E, Jennewein MF, MacCamy AJ, et al. (2021). mRNA vaccination boosts cross-variant
902 neutralizing antibodies elicited by SARS-CoV-2 infection. Science. 2021/03/27.
903 11. Cele S, Gazy I, Jackson L, Hwa SH, Tegally H, Lustig G, Giandhari J, Pillay S, Wilkinson
904 E, Naidoo Y, et al. (2021). Escape of SARS-CoV-2 501Y.V2 from neutralization by convalescent
905 plasma. Nature. 2021/03/30.
906 12. Hoffmann M, Arora P, Gross R, Seidel A, Hornich BF, Hahn AS, Kruger N, Graichen L,
907 Hofmann-Winkler H, Kempf A, et al. (2021). SARS-CoV-2 variants B.1.351 and P.1 escape from
908 neutralizing antibodies. Cell. 2021/04/02.
909 13. Planas D, Bruel T, Grzelak L, Guivel-Benhassine F, Staropoli I, Porrot F, Planchais C,
910 Buchrieser J, Rajah MM, Bishop E, et al. (2021). Sensitivity of infectious SARS-CoV-2 B.1.1.7
911 and B.1.351 variants to neutralizing antibodies. Nat Med. 2021/03/28.
912 14. Edara VV, Norwood C, Floyd K, Lai L, Davis-Gardner ME, Hudson WH, Mantus G, Nyhoff
913 LE, Adelman MW, Fineman R, et al. (2021). Infection- and vaccine-induced antibody binding and
914 neutralization of the B.1.351 SARS-CoV-2 variant. Cell Host Microbe 29, 516-521 e513.
915 2021/04/03.
916 15. Kuzmina A, Khalaila Y, Voloshin O, Keren-Naus A, Boehm-Cohen L, Raviv Y, Shemer-
917 Avni Y, Rosenberg E and Taube R. (2021). SARS-CoV-2 spike variants exhibit differential
918 infectivity and neutralization resistance to convalescent or post-vaccination sera. Cell Host
919 Microbe 29, 522-528 e522. 2021/04/01.
920 16. Skelly DT, Harding AC, Gilbert-Jaramillo J, Knight ML, Longet S, Brown A, Adele S,
921 Adland E, Brown H, Team ML, et al. (2021). Vaccine-induced immunity provides more robust

922 heterotypic immunity than natural infection to emerging SARS-CoV-2 variants of concern.
923 Research Square.
924 17. Tarke A, Sidney J, Methot N, Zhang Y, Dan JM, Goodwin B, Rubiro P, Sutherland A, da
925 Silva Antunes R, Frazier A, et al. (2021). Negligible impact of SARS-CoV-2 variants on CD4 (+)
926 and CD8 (+) T cell reactivity in COVID-19 exposed donors and vaccinees. bioRxiv. 2021/03/11.
927 18. Redd AD, Nardin A, Kared H, Bloch EM, Pekosz A, Laeyendecker O, Abel B, Fehlings M,
928 Quinn TC and Tobian AA. (2021). CD8+ T cell responses in COVID-19 convalescent individuals
929 target conserved epitopes from multiple prominent SARS-CoV-2 circulating variants. medRxiv.
930 2021/02/18.
931 19. Geers D, Shamier MC, Bogers S, den Hartog G, Gommers L, Nieuwkoop NN, Schmitz
932 KS, Rijsbergen LC, van Osch JAT, Dijkhuizen E, et al. (2021). SARS-CoV-2 variants of concern
933 partially escape humoral but not T-cell responses in COVID-19 convalescent donors and
934 vaccinees. Sci Immunol 6. 2021/05/27.
935 20. Woldemeskel BA, Garliss CC and Blankson JN. (2021). SARS-CoV-2 mRNA vaccines
936 induce broad CD4+ T cell responses that recognize SARS-CoV-2 variants and HCoV-NL63. J
937 Clin Invest 131. 2021/04/07.
938 21. Stankov MV, Cossmann A, Bonifacius A, Dopfer-Jablonka A, Ramos GM, Godecke N,
939 Scharff AZ, Happle C, Boeck AL, Tran AT, et al. (2021). Humoral and cellular immune responses
940 against SARS-CoV-2 variants and human coronaviruses after single BNT162b2 vaccination. Clin
941 Infect Dis. 2021/06/17.
942 22. Tauzin A, Nayrac M, Benlarbi M, Gong SY, Gasser R, Beaudoin-Bussieres G, Brassard
943 N, Laumaea A, Vezina D, Prevost J, et al. (2021). A single dose of the SARS-CoV-2 vaccine
944 BNT162b2 elicits Fc-mediated antibody effector functions and T cell responses. Cell Host Microbe
945 29, 1137-1150 e1136. 2021/06/17.

946 23. Chen G, Wu D, Guo W, Cao Y, Huang D, Wang H, Wang T, Zhang X, Chen H, Yu H, et
947 al. (2020). Clinical and immunological features of severe and moderate coronavirus disease 2019.
948 J Clin Invest 130, 2620-2629. 2020/03/29.
949 24. Woodruff MC, Ramonell RP, Nguyen DC, Cashman KS, Saini AS, Haddad NS, Ley AM,
950 Kyu S, Howell JC, Ozturk T, et al. (2020). Extrafollicular B cell responses correlate with
951 neutralizing antibodies and morbidity in COVID-19. Nat Immunol 21, 1506-1516. 2020/10/09.
952 25. Rydyznski Moderbacher C, Ramirez SI, Dan JM, Grifoni A, Hastie KM, Weiskopf D,
953 Belanger S, Abbott RK, Kim C, Choi J, et al. (2020). Antigen-Specific Adaptive Immunity to SARS-
954 CoV-2 in Acute COVID-19 and Associations with Age and Disease Severity. Cell 183, 996-1012
955 e1019. 2020/10/05.
956 26. Neidleman J, Luo X, George AF, McGregor M, Yang J, Yun C, Murray V, Gill G, Greene
957 WC, Vasquez J, et al. (2021). Distinctive features of SARS-CoV-2-specific T cells predict recovery
958 from severe COVID-19. Cell Rep 36, 109414. 2021/07/15.
959 27. Dan JM, Mateus J, Kato Y, Hastie KM, Yu ED, Faliti CE, Grifoni A, Ramirez SI, Haupt S,
960 Frazier A, et al. (2021). Immunological memory to SARS-CoV-2 assessed for up to 8 months after
961 infection. Science 371. 2021/01/08.
962 28. Neidleman J, Luo X, Frouard J, Xie G, Gill G, Stein ES, McGregor M, Ma T, George AF,
963 Kosters A, et al. (2020). SARS-CoV-2-Specific T Cells Exhibit Phenotypic Features of Helper
964 Function, Lack of Terminal Differentiation, and High Proliferation Potential. Cell Rep Med 1,
965 100081. 2020/08/26.
966 29. Soresina A, Moratto D, Chiarini M, Paolillo C, Baresi G, Foca E, Bezzi M, Baronio B,
967 Giacomelli M and Badolato R. (2020). Two X-linked agammaglobulinemia patients develop
968 pneumonia as COVID-19 manifestation but recover. Pediatr Allergy Immunol. 2020/04/23.
969 30. Evavold BD and Allen PM. (1991). Separation of IL-4 production from Th cell proliferation
970 by an altered T cell receptor ligand. Science 252, 1308-1310. 1991/05/31.

971 31. Sloan-Lancaster J and Allen PM. (1996). Altered peptide ligand-induced partial T cell
972 activation: molecular mechanisms and role in T cell biology. Annu Rev Immunol 14, 1-27.
973 1996/01/01.
974 32. Goel RR, Apostolidis SA, Painter MM, Mathew D, Pattekar A, Kuthuru O, Gouma S, Hicks
975 P, Meng W, Rosenfeld AM, et al. (2021). Distinct antibody and memory B cell responses in SARS-
976 CoV-2 naive and recovered individuals following mRNA vaccination. Sci Immunol 6. 2021/04/17.
977 33. Ebinger JE, Fert-Bober J, Printsev I, Wu M, Sun N, Figueiredo JC, Eyk JEV, Braun JG,
978 Cheng S and Sobhani K. (2021). Prior COVID-19 Infection and Antibody Response to Single
979 Versus Double Dose mRNA SARS-CoV-2 Vaccination. medRxiv. 2021/03/04.
980 34. Ritchie ME, Phipson B, Wu D, Hu Y, Law CW, Shi W and Smyth GK. (2015). limma powers
981 differential expression analyses for RNA-sequencing and microarray studies. Nucleic Acids Res
982 43, e47. 2015/01/22.
983 35. Kaech SM, Tan JT, Wherry EJ, Konieczny BT, Surh CD and Ahmed R. (2003). Selective
984 expression of the interleukin 7 receptor identifies effector CD8 T cells that give rise to long-lived
985 memory cells. Nat Immunol 4, 1191-1198.
986 36. Gupta RK. (2021). Will SARS-CoV-2 variants of concern affect the promise of vaccines?
987 Nat Rev Immunol. 2021/05/01.
988 37. Madhi SA, Baillie V, Cutland CL, Voysey M, Koen AL, Fairlie L, Padayachee SD, Dheda
989 K, Barnabas SL, Bhorat QE, et al. (2021). Efficacy of the ChAdOx1 nCoV-19 Covid-19 Vaccine
990 against the B.1.351 Variant. N Engl J Med. 2021/03/17.
991 38. Abu-Raddad LJ, Chemaitelly H, Butt AA and National Study Group for C-V. (2021).
992 Effectiveness of the BNT162b2 Covid-19 Vaccine against the B.1.1.7 and B.1.351 Variants. N
993 Engl J Med. 2021/05/06.
994 39. Klenerman P and Zinkernagel RM. (1998). Original antigenic sin impairs cytotoxic T
995 lymphocyte responses to viruses bearing variant epitopes. Nature 394, 482-485. 1998/08/11.

996 40. Lederer K, Castano D, Gomez Atria D, Oguin TH, 3rd, Wang S, Manzoni TB, Muramatsu
997 H, Hogan MJ, Amanat F, Cherubin P, et al. (2020). SARS-CoV-2 mRNA Vaccines Foster Potent
998 Antigen-Specific Germinal Center Responses Associated with Neutralizing Antibody Generation.
999 Immunity 53, 1281-1295 e1285. 2020/12/10.
1000 41. Bacchus-Souffan C, Fitch M, Symons J, Abdel-Mohsen M, Reeves DB, Hoh R, Stone M,
1001 Hiatt J, Kim P, Chopra A, et al. (2021). Relationship between CD4 T cell turnover, cellular
1002 differentiation and HIV persistence during ART. PLoS Pathog 17, e1009214. 2021/01/20.
1003 42. Ma T, Ryu H, McGregor M, Babcock B, Neidleman J, Xie G, George AF, Frouard J, Murray
1004 V, Gill G, et al. (2021). Protracted yet coordinated differentiation of long-lived SARS-CoV-2-
1005 specific CD8+ T cells during COVID-19 convalescence. bioRxiv 2021.04.28.441880.
1006 43. Mamazhakypov A, Viswanathan G, Lawrie A, Schermuly RT and Rajagopal S. (2019).
1007 The role of chemokines and chemokine receptors in pulmonary arterial hypertension. Br J
1008 Pharmacol 178, 72-89. 2019/08/11.
1009 44. Newell EW, Sigal N, Nair N, Kidd BA, Greenberg HB and Davis MM. (2013). Combinatorial
1010 tetramer staining and mass cytometry analysis facilitate T-cell epitope mapping and
1011 characterization. Nat Biotechnol 31, 623-629. 2013/06/12.
1012 45. Ma T, Luo X, George AF, Mukherjee G, Sen N, Spitzer TL, Giudice LC, Greene WC and
1013 Roan NR. (2020). HIV efficiently infects T cells from the endometrium and remodels them to
1014 promote systemic viral spread. Elife 9, e55487. 2020/05/27.
1015 46. Cavrois M, Banerjee T, Mukherjee G, Raman N, Hussien R, Rodriguez BA, Vasquez J,
1016 Spitzer MH, Lazarus NH, Jones JJ, et al. (2017). Mass Cytometric Analysis of HIV Entry,
1017 Replication, and Remodeling in Tissue CD4+ T Cells. Cell Rep 20, 984-998.
1018 47. Neidleman J, Luo X, Frouard J, Xie G, Hsiao F, Ma T, Morcilla V, Lee A, Telwatte S,
1019 Thomas R, et al. (2020). Phenotypic analysis of the unstimulated in vivo HIV CD4 T cell reservoir.
1020 Elife 9, e55487. 2020/09/30.

1021 48. Xie G, Luo X, Ma T, Frouard J, Neidleman J, Hoh R, Deeks SG, Greene WC and Roan
1022 NR. (2021). Characterization of HIV-induced remodeling reveals differences in infection
1023 susceptibility of memory CD4(+) T cell subsets in vivo. Cell Rep 35, 109038. 2021/04/29.
1024 49. Nowicka M, Krieg C, Crowell HL, Weber LM, Hartmann FJ, Guglietta S, Becher B,
1025 Levesque MP and Robinson MD. (2017). CyTOF workflow: differential discovery in high-
1026 throughput high-dimensional cytometry datasets. F1000Res 6, 748. 2017/05/26.
1027 50. Van Gassen S, Callebaut B, Van Helden MJ, Lambrecht BN, Demeester P, Dhaene T and
1028 Saeys Y. (2015). FlowSOM: Using self-organizing maps for visualization and interpretation of
1029 cytometry data. Cytometry A 87, 636-645. 2015/01/13.
1030 51. Wilkerson MD and Hayes DN. (2010). ConsensusClusterPlus: a class discovery tool with
1031 confidence assessments and item tracking. Bioinformatics 26, 1572-1573. 2010/04/30.
1032

Figure 1

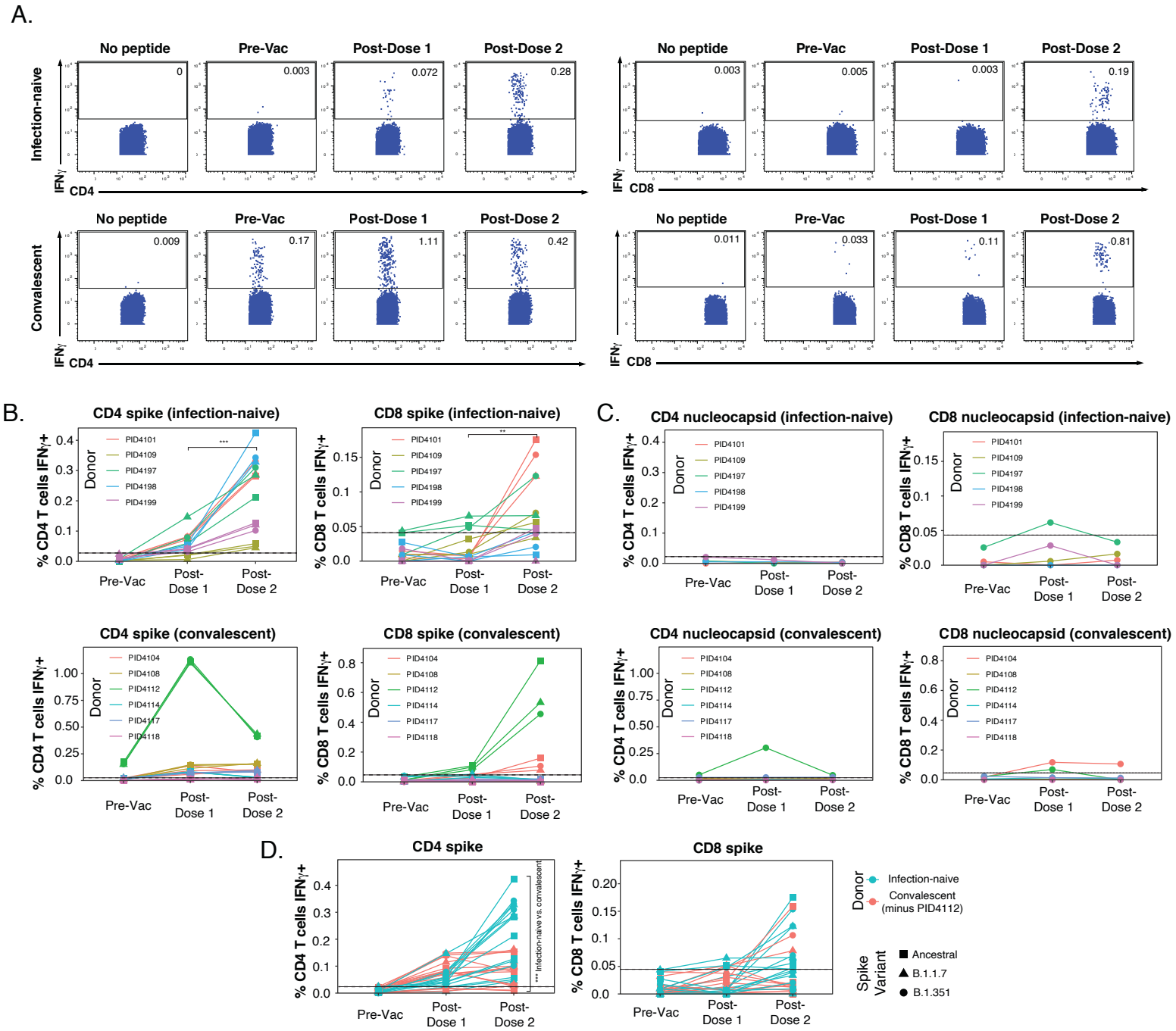
A.
No peptide
Pre-Vac
Post-Dose 1
Post-Dose 2
Infection-naive
Convalescent
IFNγ
CD4
CD8
0
0.003
0.072
0.28
0.005
0.19
0.009
0.17
1.11
0.42
0.011
0.033
0.11
0.81
B.
CD4 spike (infection-naive)
CD8 spike (infection-naive)
C.
CD4 nucleocapsid (infection-naive)
CD8 nucleocapsid (infection-naive)
CD4 spike (convalescent)
CD8 spike (convalescent)
CD4 nucleocapsid (convalescent)
CD8 nucleocapsid (convalescent)
% CD4 T cells IFNγ+
% CD8 T cells IFNγ+
Donor
PID4101
PID4109
PID4197
PID4198
PID4199
PID4104
PID4108
PID4112
PID4114
PID4117
PID4118
Pre-Vac
Post-Dose 1
Post-Dose 2
D.
CD4 spike
CD8 spike
*** Infection-naive vs. convalescent
Infection-naive
Convalescent (minus PID4112)
Spike Variant
Ancestral
B.1.1.7
B.1.351

Figure 2

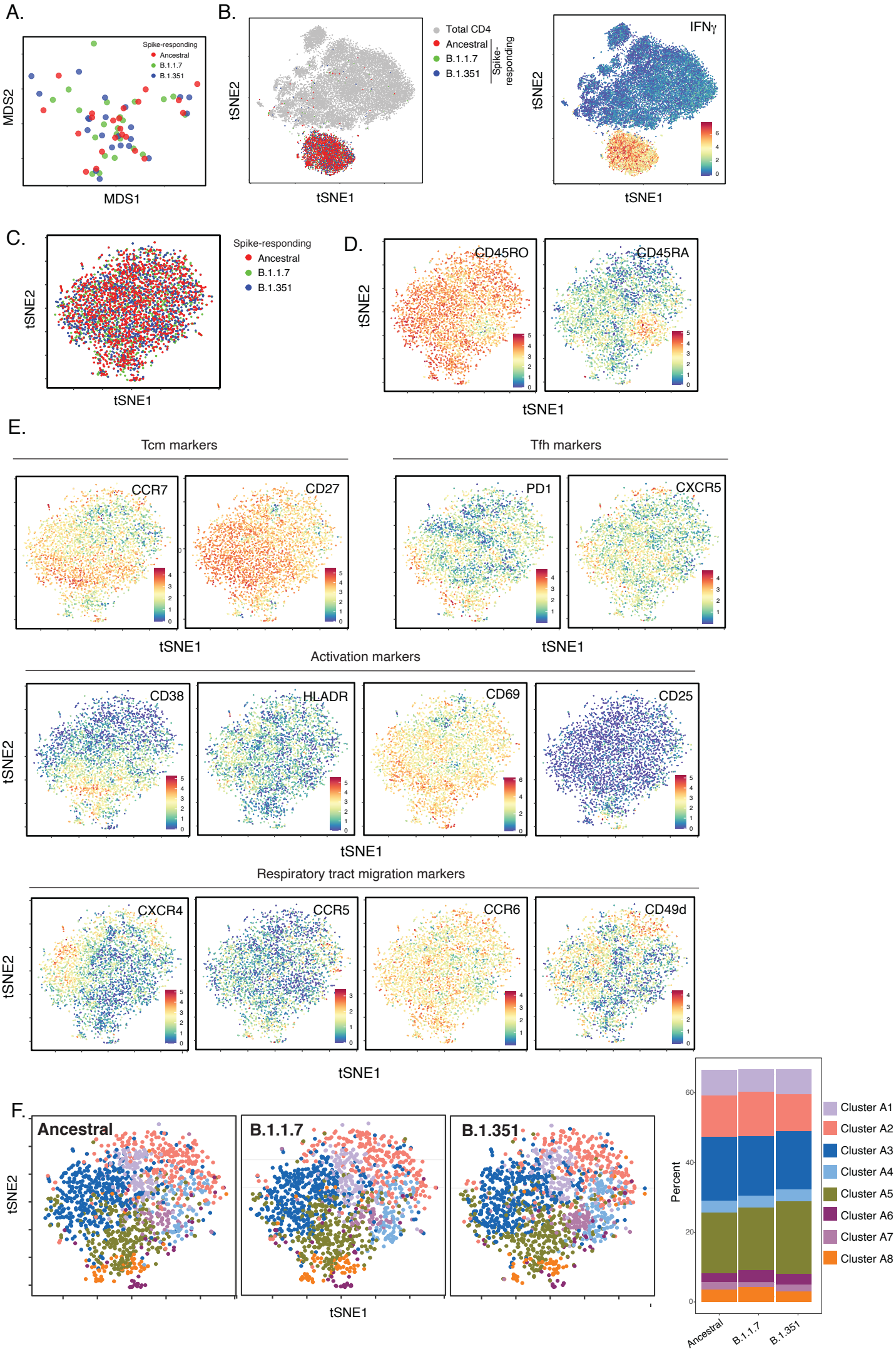
A.
Spike-responding
Ancestral
B.1.1.7
B.1.351
MDS2
MDS1
B.
Total CD4
Ancestral
B.1.1.7
B.1.351
Spike-responding
tSNE2
tSNE1
IFNγ
tSNE2
tSNE1
C.
Spike-responding
Ancestral
B.1.1.7
B.1.351
tSNE2
tSNE1
D.
CD45RO
CD45RA
tSNE2
tSNE1
E.
Tcm markers
CCR7
CD27
tSNE1
Tfh markers
PD1
CXCR5
tSNE1
Activation markers
CD38
HLADR
CD69
CD25
tSNE2
tSNE1
Respiratory tract migration markers
CXCR4
CCR5
CCR6
CD49d
tSNE2
tSNE1
F.
Ancestral
B.1.1.7
B.1.351
tSNE2
tSNE1
Percent
Cluster A1
Cluster A2
Cluster A3
Cluster A4
Cluster A5
Cluster A6
Cluster A7
Cluster A8
Ancestral
B.1.1.7
B.1.351

Figure 3

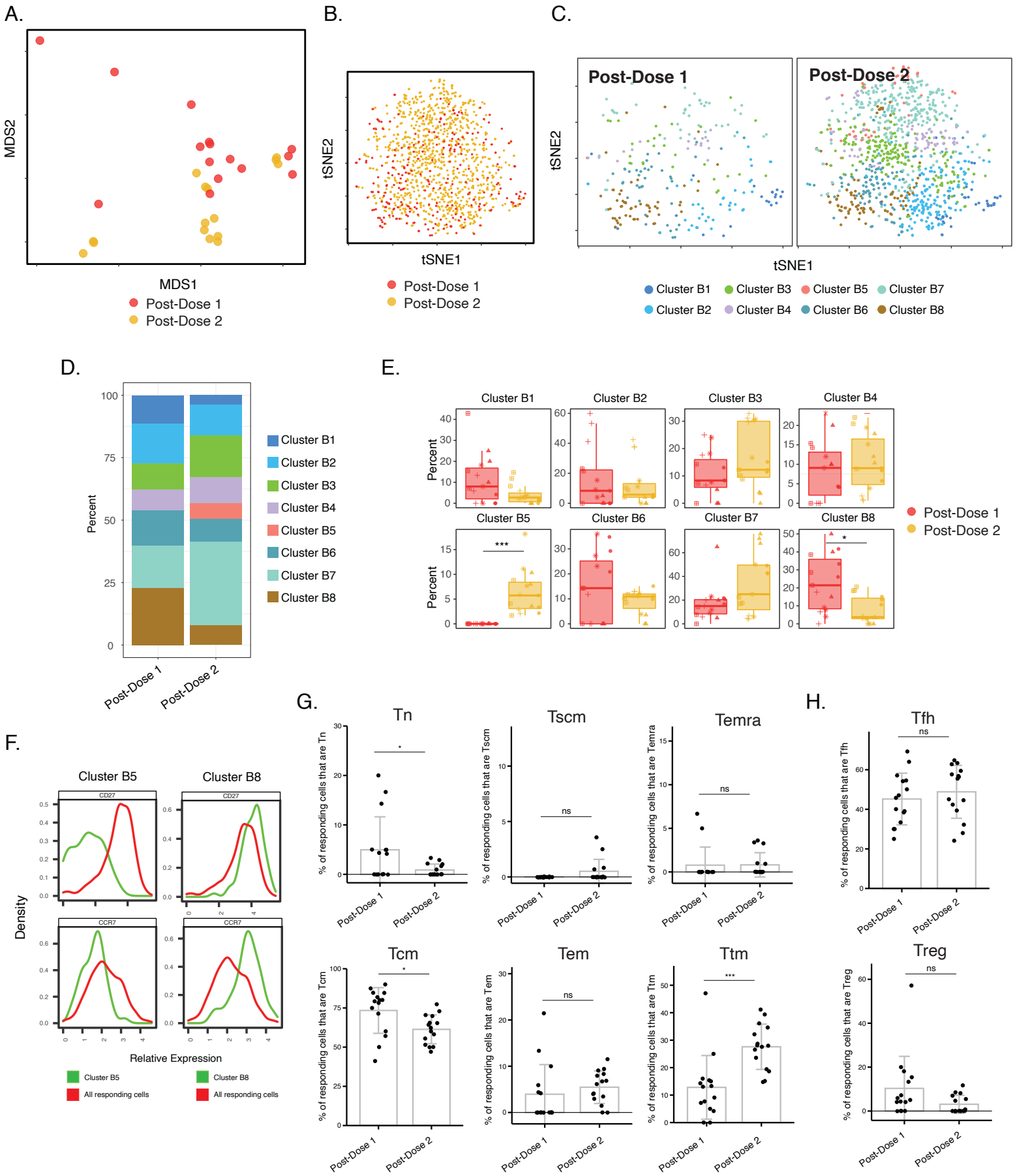
A.
MDS2
MDS1
Post-Dose 1
Post-Dose 2
B.
tSNE2
tSNE1
Post-Dose 1
Post-Dose 2
C.
Post-Dose 1
Post-Dose 2
tSNE2
tSNE1
Cluster B1
Cluster B2
Cluster B3
Cluster B4
Cluster B5
Cluster B6
Cluster B7
Cluster B8
D.
Percent
Post-Dose 1
Post-Dose 2
E.
Cluster B1
Cluster B2
Cluster B3
Cluster B4
Cluster B5
Cluster B6
Cluster B7
Cluster B8
Percent
Post-Dose 1
Post-Dose 2
F.
Cluster B5
Cluster B8
CD27
CCR7
Density
Relative Expression
Cluster B5
All responding cells
Cluster B8
All responding cells
G.
Tn
Tscm
Temra
Tcm
Tem
Ttm
% of responding cells that are Tn
% of responding cells that are Tscm
% of responding cells that are Temra
% of responding cells that are Tcm
% of responding cells that are Tem
% of responding cells that are Ttm
Post-Dose 1
Post-Dose 2
H.
Tfh
Treg
% of responding cells that are Tfh
% of responding cells that are Treg
Post-Dose 1
Post-Dose 2

Figure 4

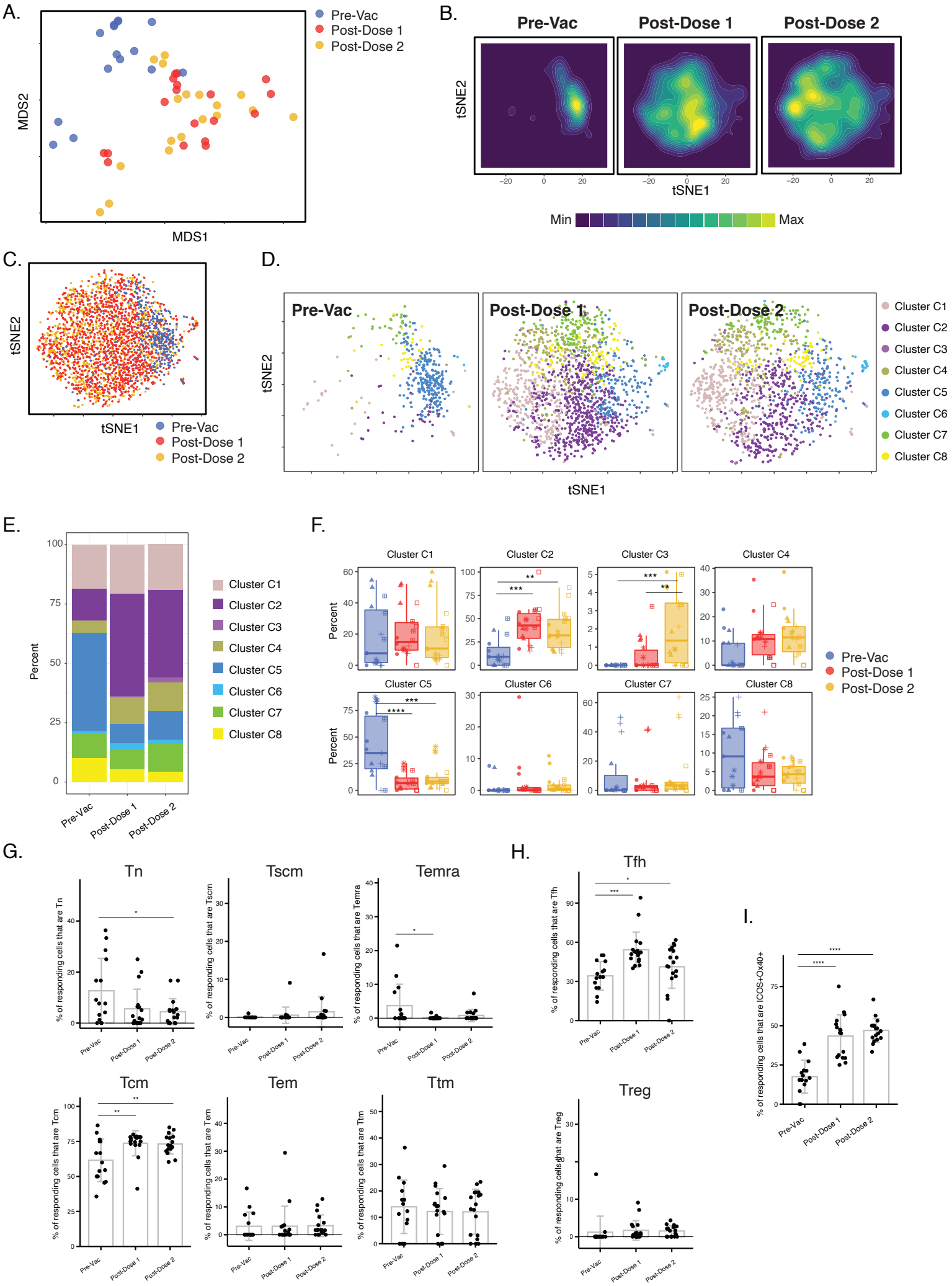
A.
Pre-Vac
Post-Dose 1
Post-Dose 2
MDS2
MDS1
B.
Pre-Vac
Post-Dose 1
Post-Dose 2
tSNE2
tSNE1
Min
Max
C.
tSNE2
tSNE1
Pre-Vac
Post-Dose 1
Post-Dose 2
D.
Pre-Vac
Post-Dose 1
Post-Dose 2
tSNE2
tSNE1
Cluster C1
Cluster C2
Cluster C3
Cluster C4
Cluster C5
Cluster C6
Cluster C7
Cluster C8
E.
Percent
Pre-Vac
Post-Dose 1
Post-Dose 2
F.
Cluster C1
Cluster C2
Cluster C3
Cluster C4
Cluster C5
Cluster C6
Cluster C7
Cluster C8
Percent
Pre-Vac
Post-Dose 1
Post-Dose 2
G.
Tn
Tscm
Temra
Tcm
Tem
Ttm
% of responding cells that are Tn
% of responding cells that are Tscm
% of responding cells that are Temra
% of responding cells that are Tcm
% of responding cells that are Tem
% of responding cells that are Ttm
H.
Tfh
Treg
% of responding cells that are Tfh
% of responding cells that are Treg
I.
% of responding cells that are ICOS+Ox40+

Figure 5

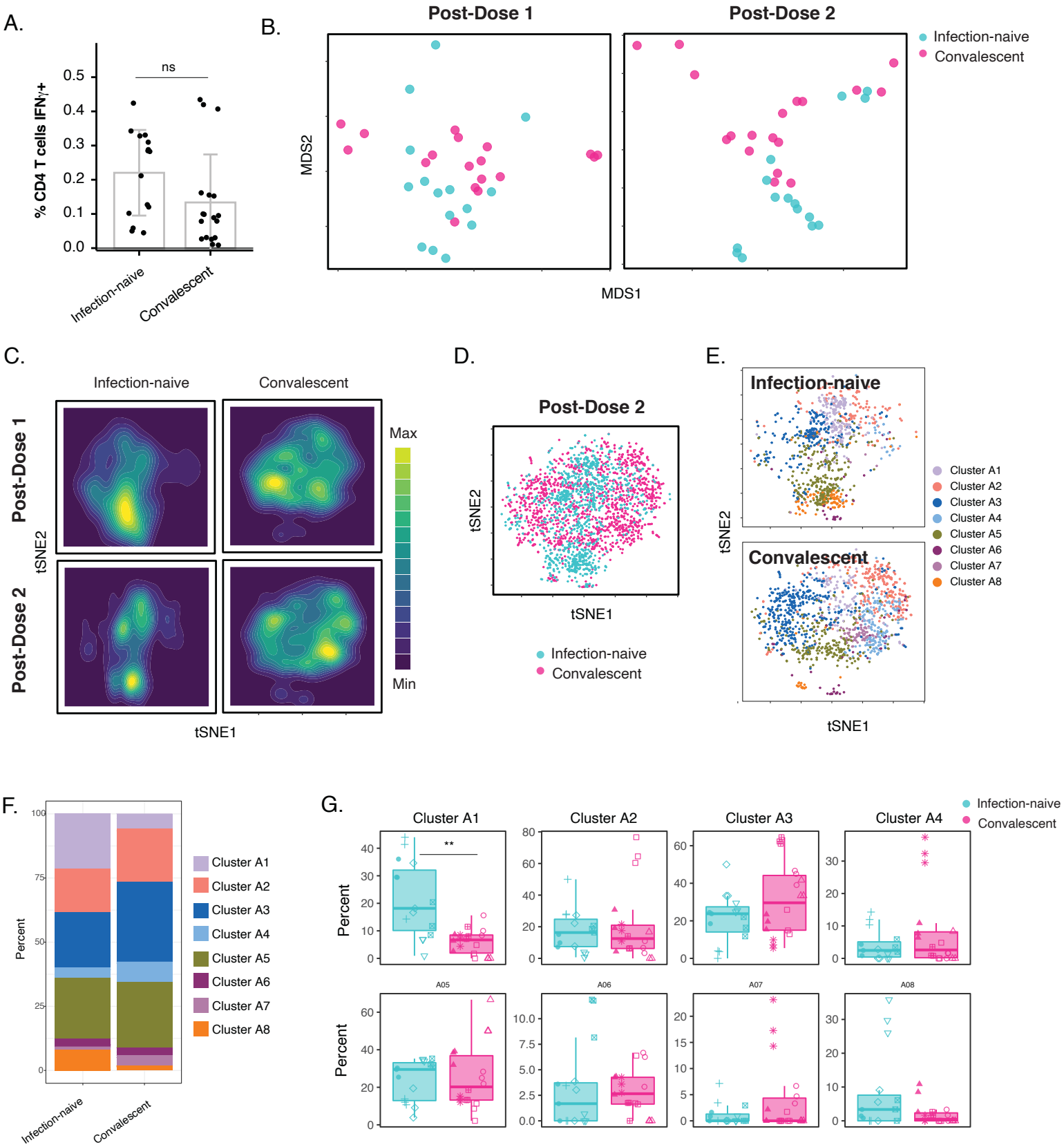
A.
% CD4 T cells IFNγ+
ns
Infection-naive
Convalescent
B.
Post-Dose 1
Post-Dose 2
MDS2
MDS1
Infection-naive
Convalescent
C.
Infection-naive
Convalescent
Post-Dose 1
Post-Dose 2
tSNE2
tSNE1
Max
Min
D.
Post-Dose 2
tSNE2
tSNE1
Infection-naive
Convalescent
E.
Infection-naive
Convalescent
tSNE2
tSNE1
Cluster A1
Cluster A2
Cluster A3
Cluster A4
Cluster A5
Cluster A6
Cluster A7
Cluster A8
F.
Percent
Infection-naive
Convalescent
Cluster A1
Cluster A2
Cluster A3
Cluster A4
Cluster A5
Cluster A6
Cluster A7
Cluster A8
G.
Cluster A1
Cluster A2
Cluster A3
Cluster A4
Infection-naive
Convalescent
Percent
**
A05
A06
A07
A08

Figure 6

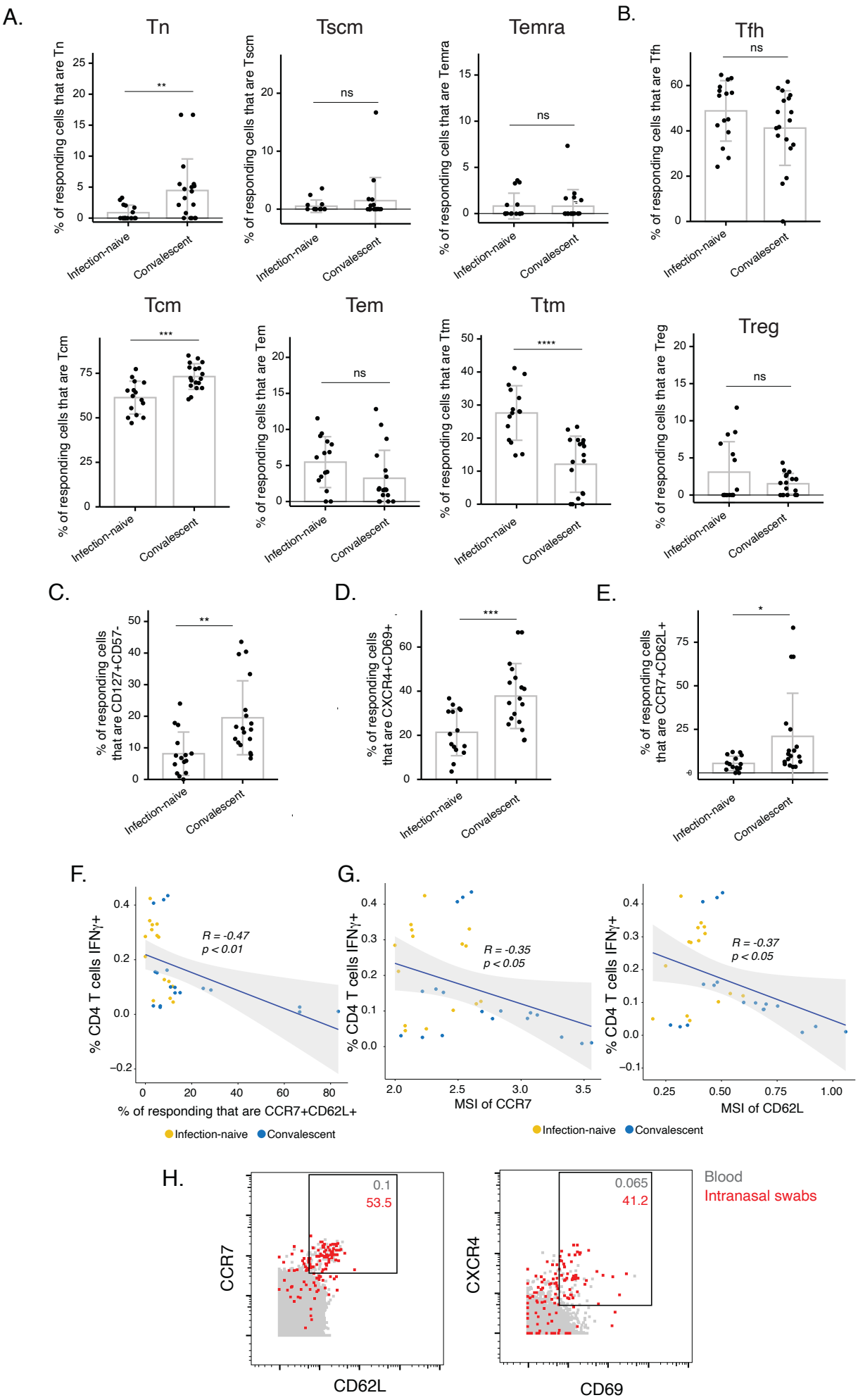
A.
Tn
Tscm
Temra
B.
Tfh
Tcm
Tem
Ttm
Treg
% of responding cells that are Tn
% of responding cells that are Tscm
% of responding cells that are Temra
% of responding cells that are Tfh
% of responding cells that are Tcm
% of responding cells that are Tem
% of responding cells that are Ttm
% of responding cells that are Treg
Infection-naive
Convalescent
ns
C.
D.
E.
% of responding cells that are CD127+CD57-
% of responding cells that are CXCR4+CD69+
% of responding cells that are CCR7+CD62L+
F.
G.
% CD4 T cells IFNγ+
R = -0.47
p < 0.01
% of responding that are CCR7+CD62L+
R = -0.35
p < 0.05
MSI of CCR7
R = -0.37
p < 0.05
MSI of CD62L
H.
CCR7
CD62L
0.1
53.5
CXCR4
CD69
0.065
41.2
Blood
Intranasal swabs

Figure S1

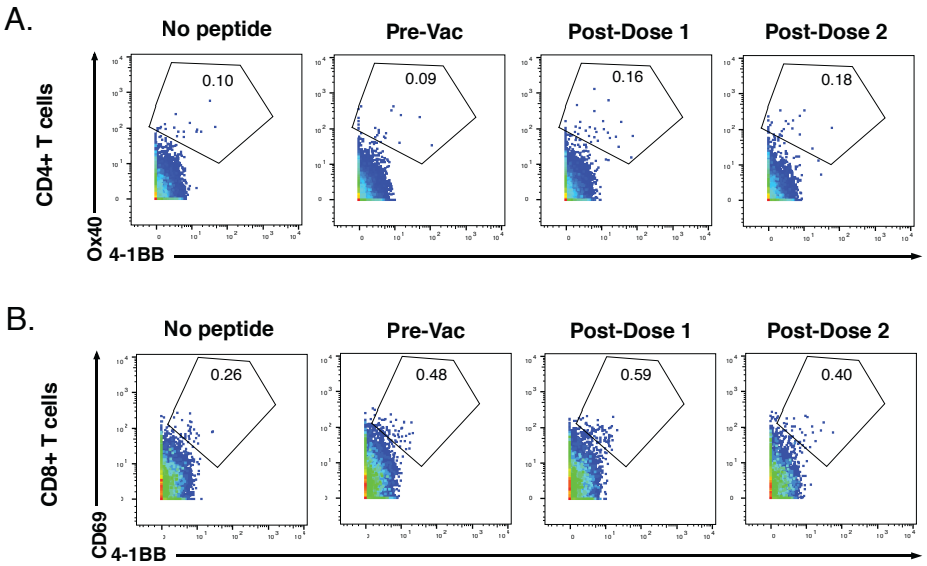
A.
No peptide
Pre-Vac
Post-Dose 1
Post-Dose 2
CD4+ T cells
0.10
0.09
0.16
0.18
Ox40
4-1BB
B.
No peptide
Pre-Vac
Post-Dose 1
Post-Dose 2
CD8+ T cells
0.26
0.48
0.59
0.40
CD69
4-1BB

Figure S2

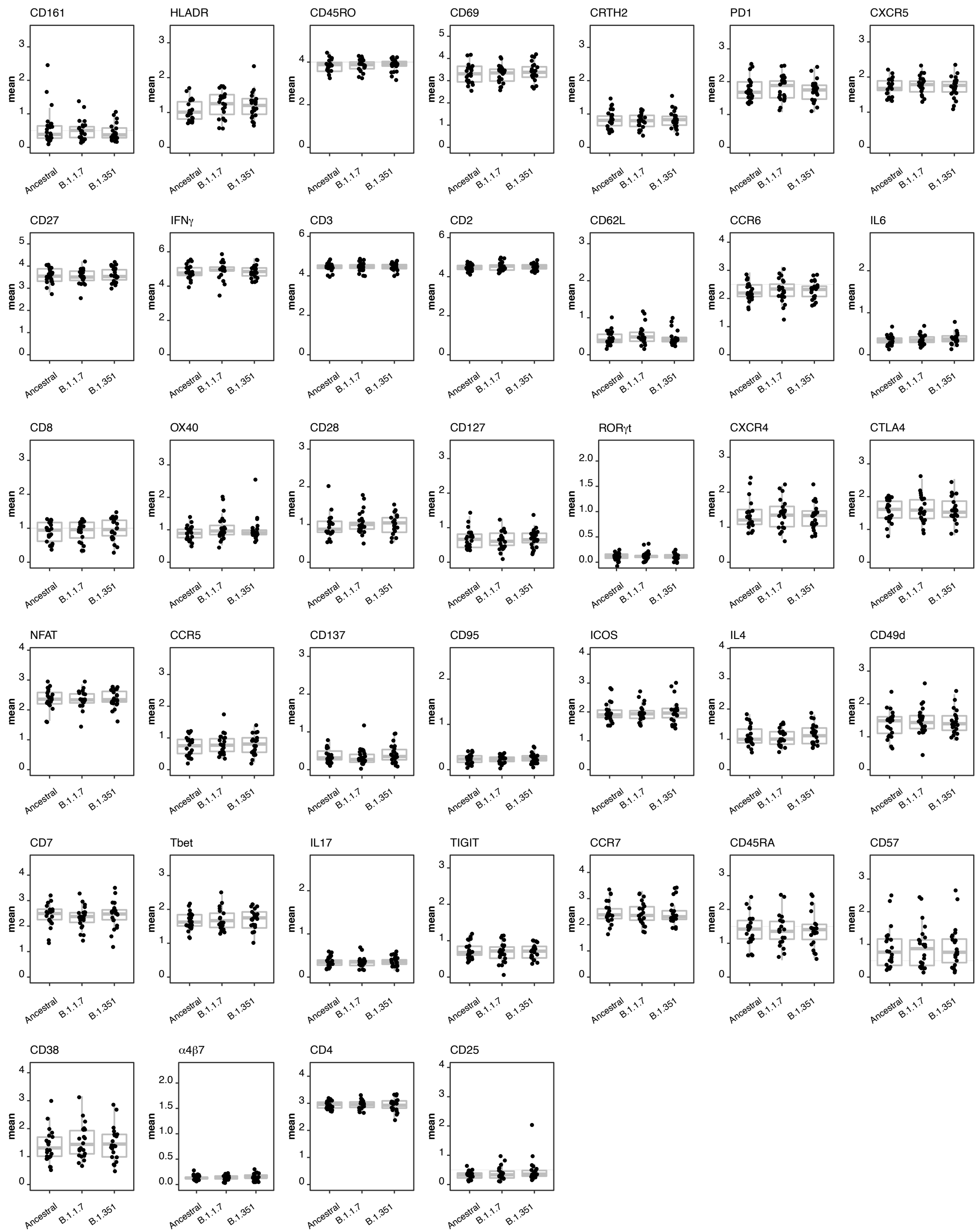
CD161
HLADR
CD45RO
CD69
CRTH2
PD1
CXCR5
CD27
IFNγ
CD3
CD2
CD62L
CCR6
IL6
CD8
OX40
CD28
CD127
RORγt
CXCR4
CTLA4
NFAT
CCR5
CD137
CD95
ICOS
IL4
CD49d
CD7
Tbet
IL17
TIGIT
CCR7
CD45RA
CD57
CD38
α4β7
CD4
CD25
mean
Ancestral
B.1.1.7
B.1.351

Figure S3

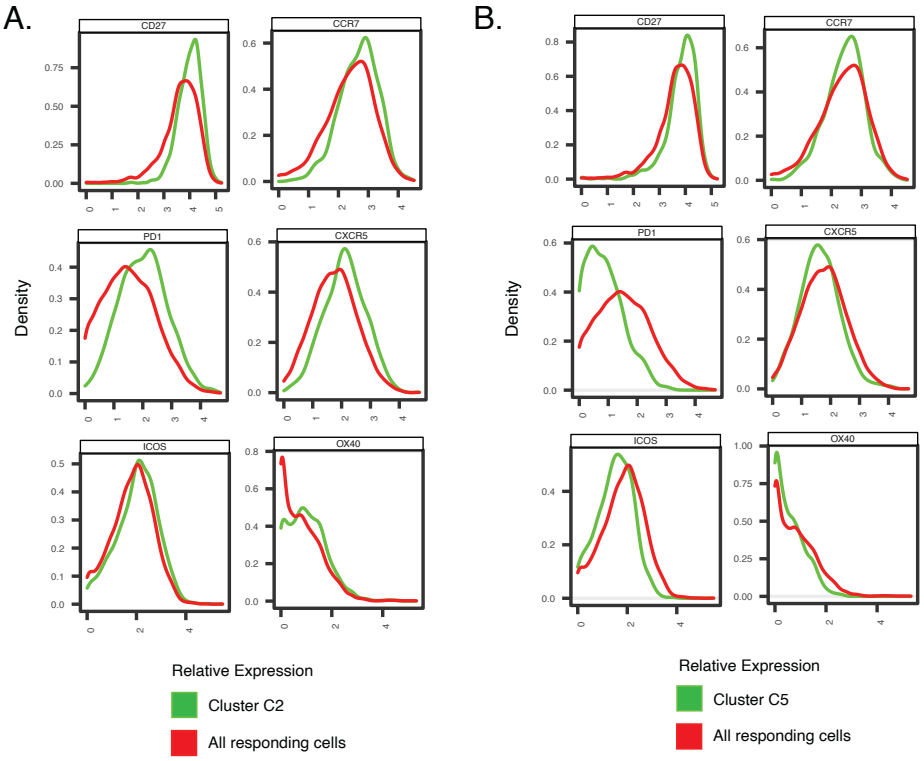
A.
B.
CD27
CCR7
PD1
CXCR5
ICOS
OX40
Density
Relative Expression
Cluster C2
All responding cells
Relative Expression
Cluster C5
All responding cells

Figure S4

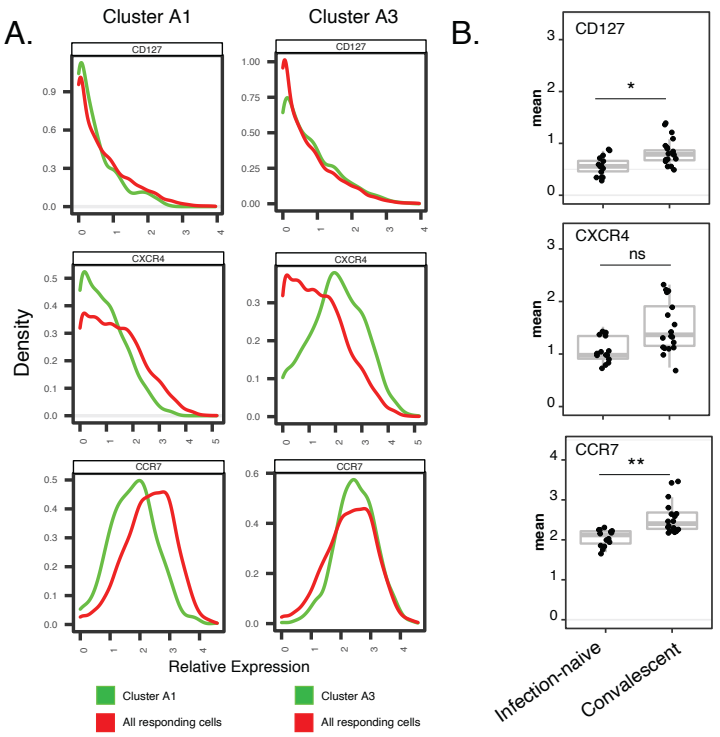
A.
Cluster A1
Cluster A3
CD127
CXCR4
CCR7
Density
Relative Expression
Cluster A1
All responding cells
Cluster A3
All responding cells
B.
CD127
CXCR4
CCR7
mean
*
ns
**
Infection-naive
Convalescent

Figure S5

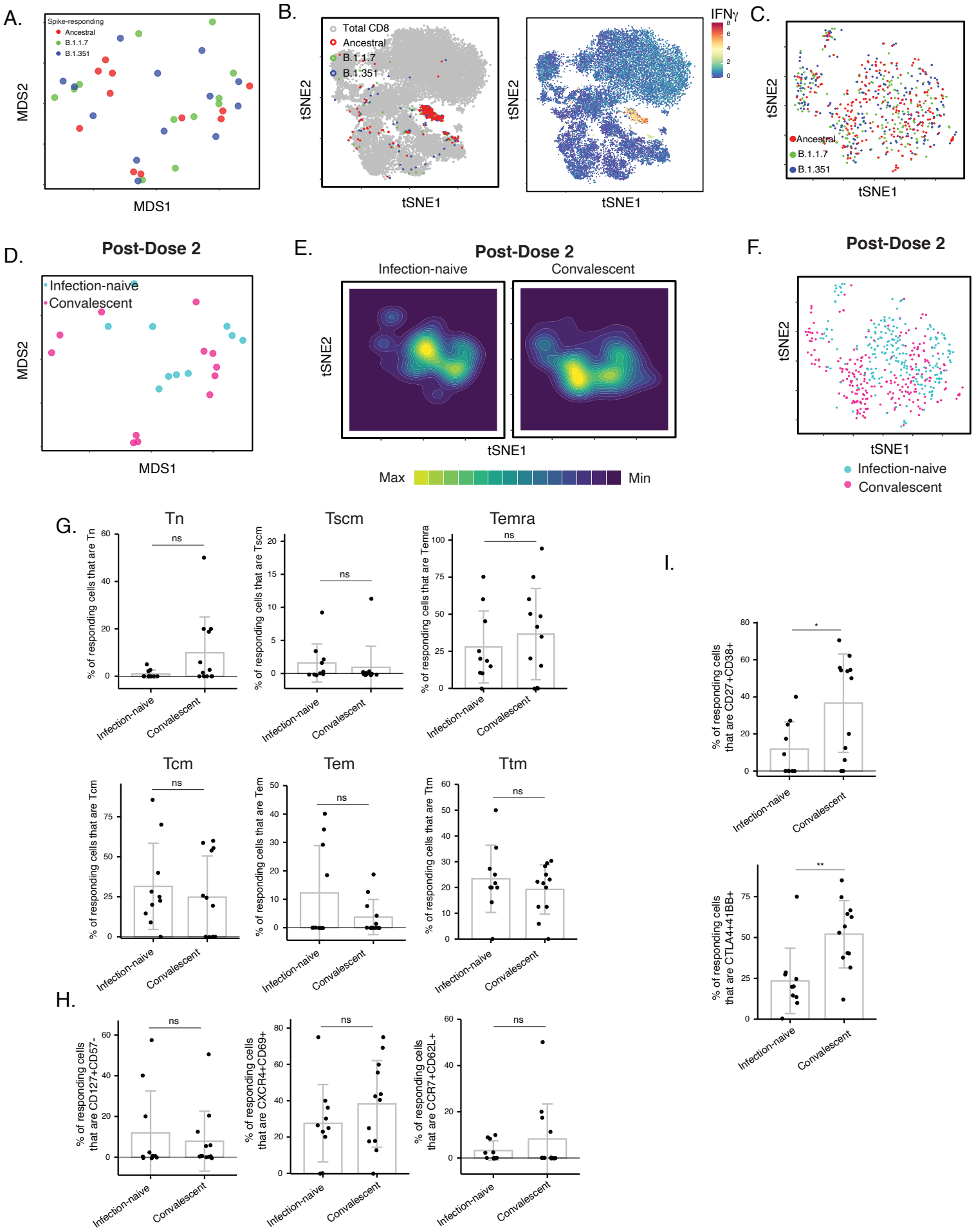
A.
Spike-responding
Ancestral
B.1.1.7
B.1.351
MDS2
MDS1
B.
Total CD8
Ancestral
B.1.1.7
B.1.351
tSNE2
tSNE1
IFNγ
C.
Ancestral
B.1.1.7
B.1.351
D.
Post-Dose 2
Infection-naive
Convalescent
E.
Post-Dose 2
Infection-naive
Convalescent
Max
Min
F.
Post-Dose 2
Infection-naive
Convalescent
G.
Tn
Tscm
Temra
Tcm
Tem
Ttm
% of responding cells that are Tn
% of responding cells that are Tscm
% of responding cells that are Temra
% of responding cells that are Tcm
% of responding cells that are Tem
% of responding cells that are Ttm
ns
H.
% of responding cells that are CD127+CD57-
% of responding cells that are CXCR4+CD69+
% of responding cells that are CCR7+CD62L+
I.
% of responding cells that are CD27+CD38+
% of responding cells that are CTLA4+41BB+
*
**